MISCELLANEOUS PAPER S-78-14

AN ELASTIC-PLASTIC CONSTITUTIVE RELATION FOR TRANSVERSE-ISOTROPIC THREE-PHASE EARTH MATERIALS

by

George Y. Baladi

Geotechnical Laboratory
U. S. Army Engineer Waterways Experiment Station
P. O. Box 631, Vicksburg, Miss. 39180

August 1978
Final Report

Prepared for Assistant Secretary of the Army (R&D)
Department of the Army
Washington D. C. 20310

Under Project No. 4A161101A91D

Destroy this report when no longer needed. Do not return it to the originator.

Unclassified

SECURITY CLASSIFICATION OF THIS PAGE (When Data Entered)

REPORT DOCUMENTATION PAGE

READ INSTRUCTIONS BEFORE COMPLETING FORM

1. REPORT NUMBER: Miscellaneous Paper S-78-14
2. GOVT ACCESSION NO.
3. RECIPIENT'S CATALOG NUMBER

4. TITLE (and Subtitle): AN ELASTIC-PLASTIC CONSTITUTIVE RELATION FOR TRANSVERSE-ISOTROPIC THREE-PHASE EARTH MATERIALS
5. TYPE OF REPORT & PERIOD COVERED: Final Report
6. PERFORMING ORG. REPORT NUMBER

7. AUTHOR(s): George Y. Baladi
8. CONTRACT OR GRANT NUMBER(s): Project No. 4A161101A91D

9. PERFORMING ORGANIZATION NAME AND ADDRESS
U. S. Army Engineer Waterways Experiment Station
Geotechnical Laboratory
P. O. Box 631, Vicksburg, Miss. 39180

10. PROGRAM ELEMENT, PROJECT, TASK AREA & WORK UNIT NUMBERS

11. CONTROLLING OFFICE NAME AND ADDRESS
Assistant Secretary of the Army (R&D)
Department of the Army
Washington, D. C. 20310

12. REPORT DATE: August 1978
13. NUMBER OF PAGES: 82

14. MONITORING AGENCY NAME & ADDRESS (if different from Controlling Office)

15. SECURITY CLASS. (of this report): Unclassified
15a. DECLASSIFICATION/DOWNGRADING SCHEDULE

16. DISTRIBUTION STATEMENT (of this Report)

Approved for public release; distribution unlimited.

87 p.

17. DISTRIBUTION STATEMENT (of the abstract entered in Block 20, if different from Report)

WES-MP-S-78-14

18. SUPPLEMENTARY NOTES

This work was sponsored by the Assistant Secretary of the Army (R&D) under Department of the Army Project No. 4A161101A91D, In-House Laboratory Independent Research (ILIR) Program.

19. KEY WORDS (Continue on reverse side if necessary and identify by block number)

Anisotropy	Saturated soils
Constitutive models	Stress-strain relations
Elastic media	Three-phase media
Elastic plastic behavior	Transverse-isotropic materials

20. ABSTRACT (Continue on reverse side if necessary and identify by block number)

This report documents the development of a three-dimensional, elastic-plastic work-hardening constitutive model for transverse-isotropic three-phase earth materials. This model can be used to perform effective stress analyses for boundary value problems involving fully- or partially-saturated earth materials.

Within the elastic range, the model contains three dimensionless →

(Continued)

DD FORM 1 JAN 73 1473 EDITION OF 1 NOV 65 IS OBSOLETE

Unclassified

SECURITY CLASSIFICATION OF THIS PAGE (When Data Entered)

20. ABSTRACT (Continued).

parameters and two response functions. Within the plastic range, on the other hand, it contains three dimensionless parameters and three potential functions. It is shown that the numerical values of the dimensionless elastic and plastic parameters as well as the values of the coefficients in the response and potential functions can be determined experimentally using essentially conventional laboratory testing techniques. It is also shown that the model readily reduces to its isotropic counterpart without any changes in its basic mathematical functions.

The model is capable of simulating the drained and undrained behavior of typical earth materials subjected to both spherical and deviatoric states of stress. For undrained applications, it predicts the effective stresses as well as the pore pressure.

To demonstrate these features (qualitatively), the model is examined under simulated drained and undrained triaxial test conditions. In addition, the general method for obtaining the effective stress, the pore pressure, and the total material response of a three-phase system subjected to a given total stress path is outlined.

PREFACE

This study was conducted by the U. S. Army Engineer Waterways Experiment Station (WES) under Department of the Army Project No. 4A161101A91D, In-House Laboratory Indpendent Research (ILIR) Program, sponsored by the Assistant Secretary of the Army (R&D).

The investigation was conducted by Dr. G. Y. Baladi during calendar years 1976-1978 under the general direction of Mr. J. P. Sale, Chief, Geotechnical Laboratory (GL), and Dr. J. G. Jackson, Jr., Chief, Soil Dynamics Division (SDD). Useful suggestions and comments by Drs. B. Rohani and J. S. Zelasko, SDD, are appreciated. The report was written by Dr. Baladi.

Director of WES during the course of the investigation and preparation of this report was COL J. L. Cannon, CE. Technical Director was Mr. F. R. Brown.

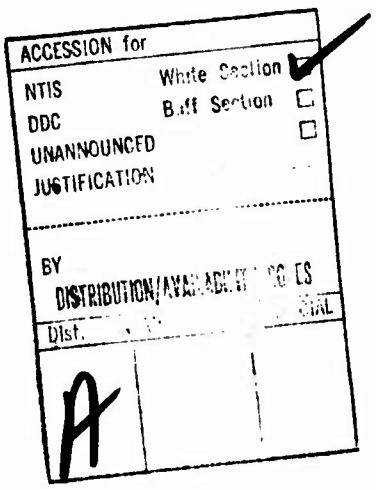

CONTENTS

AN ELASTIC-PLASTIC CONSTITUTIVE RELATION FOR TRANSVERSE-ISOTROPIC THREE-PHASE EARTH MATERIALS

PART I: INTRODUCTION

Background

1. Earth materials are multiphase systems[1] that consist in general of solid particles (possibly cemented), water and gas (air), and are often found to be inhomogeneous and anisotropic (herein the term "anisotropic" refers to the dependence of the moduli or strength of the material upon direction of loading). The intrinsic response of such materials to externally applied loads is extremely complicated. To model this response for a particular material, one must resort to the theory of continuum mechanics and have available an appropriate constitutive relation. The solution of earth structure problems then becomes a mathematical formalism that can be achieved numerically or by other means.

2. During the past few decades, the dramatic growth of computer technology and the development of new methods of numerical analysis have been paralleled by an increasing degree of complexity in material constitutive modeling. Consequently, several quite complicated elastic-ideally plastic,[2] variable moduli-type,[3-5] and elastic-plastic work-hardening[6-10] constitutive models have been developed and used by the soil and rock mechanics communities. Some of these models[6-8] are three-dimensional isotropic and/or transverse-isotropic and can predict shear-induced volume change; however, they simulate only single phase systems. The Cambridge model[9] simulates two-phase (water and solid) systems and can also predict shear-induced volume change, but it is formulated only for two-dimensional geometry, i.e., the intermediate principal stress equals either the minor or the major principal stress. In 1976, an isotropic three-dimensional two phase constitutive model for saturated cohesionless soils was developed at the U. S. Army Engineer Waterways Experiment Station (WES).[10]

3. At present, there is no single general constitutive relationship available that can simulataneously (a) be expressed in terms of a three-dimensional coordinate system, (b) apply for any state of stress and deformation, (c) simulate three-phase systems (i.e., partially saturated materials), (d) predict observed shear-induced volume change, (e) handle both isotropic and anisotropic material behavior, (f) satisfy all of the mathematical restrictions of the theory of continuous mass media, (g) derive the numerical values of the coefficients in its response and potential functions from experimental data obtained by use of essentially conventional laboratory testing techniques, and (h) be easily incorporated into contemporary finite-element and/or finite-difference computer codes. The benefits of the availability of such a constitutive relationship are obvious. It would provide a basis for the interpretation and organization of drained and undrained laboratory test data for various states of stress and deformation and provide the means (in conjunction with appropriate computer codes) to perform effective stress analyses for a wide variety of earth structures problems for either transient or static-type loading conditions.

Objective

4. The overall objective of this study was to develop a completely general, three-dimensional, elastic-plastic work-hardening constitutive relationship for transverse-isotropic three-phase earth materials. In addition, the constitutive model was desired in a form suitable for use with current finite-element and finite-difference techniques for the solution of boundary- and initial-value problems involving a variety of natural earth materials and earth structures.

Scope

5. The concepts of effective stress and material anisotropy are presented in Part II. In Part III, the development of the single-phase elastic-plastic constitutive model is presented. The application of

this model to treat multiphase systems is outlined in Part IV. The qualitive behavior of the multiphase model under triaxial test conditions is examined in Part V. Part VI summarizes key aspects of the model and furnishes recommendations for its quantitive application. Appendix A reviews basic concepts from continuum mechanics, and Appendix B describes the constitutive relations for a linear elastic transverse-isotropic material. A general description of elastic-plastic constitutive models is contained in Appendix C. Appendixes A, B, and C are included both for reference purposes and for future use. The reader is advised to read these appendixes before reading the main report.

PART II: EFFECTIVE STRESS AND ANISOTROPY CONCEPTS

6. Earth material, in its general form, is composed of a complex assemblage of discrete particles of varying shapes and orientations in a compact, possibly cemented, array. These may range in magnitude from the microscopic elements of a clay soil to the macroscopic boulders of a rock fill. The voids in the array may be filled with water or air and usually contain both. Before a constitutive model describing the behavior of these materials under an applied stress can be developed, it is necessary to consider how this stress is distributed among the several components comprising the aggregate and to understand, in general terms, the mechanical behavior of these assemblages. The emphasis throughout the remainder of this report will be on earth materials that are better described as soils than as rocks; however, the model, in principle, is applicable to both.

Effective Stress

7. The normal stress components at a point in a soil body may be divided into two parts:[11] the stress carried by the solid skeleton, referred to as the "effective stress," and the stress carried by the pore fluid, referred to as the "pore pressure." The pore pressure, in turn, must be divided into two parts: the stress carried by the water and the stress carried by the air. Mathematically, total stress* can be expressed (in indicial notation**) as[12-14]

$$\sigma_{ij} = \sigma'_{ij} + \left[P_a - \chi(P_a - P_w)\right] \delta_{ij} \qquad (1)$$

---

* Symbols used in this report are listed and defined in the Notation (Appendix D).

** Indices take on values of 1, 2, or 3. A repeated index is to be summed over its range. A comma between subscripts represents a derivative. Quantities are referred to rectangular Cartesian coordinates X_i.

where

σ_{ij} = total stress tensor

σ'_{ij} = effective stress tensor

P_a = pore air pressure

χ = dimensionless quantity proportional to the pore volume occupied by the water phase

P_w = pore water pressure

δ_{ij} = Kronecker delta = $\begin{cases} 1, & i = j \\ 0, & i \neq j \end{cases}$

Equation 1 can be rewritten as

$$\sigma_{ij} = \sigma'_{ij} + u\,\delta_{ij} \tag{2}$$

in which u is the total pore pressure representing the combined effect of the pore air pressure and the pore water pressure, i.e.,

$$u = P_a - \chi(P_a - P_w) \tag{3}$$

For a fully saturated soil, $\chi = 1$; and for a completely dry soil, $\chi = 0$.

8. For a triaxial test performed on a cylindrical specimen (r-θ-z coordinate system), the stresses are (Equation 2):

$$\sigma_z = \sigma'_z + u$$

$$\sigma_\theta = \sigma_r = \sigma'_\theta + u = \sigma'_r + u \tag{4}$$

where σ_z , σ_r and, σ_θ are, respectively, the axial, radial, and tangential total stress components. The mechanical behavior of saturated and partially saturated soils tested under triaxial conditions is discussed in the following section.

Mechanical Behavior of Soil

9. The mechanical behavior of soils subjected to externally

applied loads is quite complicated. Unlike most engineering materials, soil stress-strain properties are greatly affected by such factors as void ratio, orientation of soil particles (i.e., soil structure), degree of voids saturation, drainage conditions during loading, loading rate, loading history, and current stress state. Moreover, the effective stress is the only part of the total stress that affects soil volume changes and shear strength.

10. Figures 1 and 2, respectively, show the typical behavior of an isotropic and a transverse-isotropic soil subjected to hydrostatic stress. For the isotropic soil (Figure 1), all strains are equal under hydrostatic states of stress; however, as indicated in Figure 2, in the case of transverse-isotropic soil, the strain in the plane of isotropy, ε_r , is different from that in the axial (symmetry axis) direction, ε_z .

11. Figure 3 shows a typical variety of stress-strain-pore pressure response curves manifested by saturated anisotropic soils tested in undrained shear in a triaxial compression device* (the $r\theta$-plane is the plane of isotropy). The three specimens were first isotropically consolidated to the same effective mean normal stress level (point 2), then sheared undrained. At point 2, of course, the strain ε_r is different from the strain ε_z in each case. The shear curves marked "2 → 3" show the typical response of a normally consolidated clay or a loose sand. The curves marked "2 → 5" show behavior typical of an overconsolidated clay or a dense sand. Within the extreme limits of these loose and dense soil responses, there is a graduated response, typified herein by the curves marked "2 → 4." The latter response depends on the state of compaction (consolidation) of the material.

12. Figure 4 shows typical (qualitative) stress-strain response curves for the former anisotropic soil sheared under drained triaxial compression condition, i.e., the curves marked "1" represent dense sand or overconsolidated clay, while the curves marked "2" depict response

---

* These tests must include independent measurements of radial deformation.

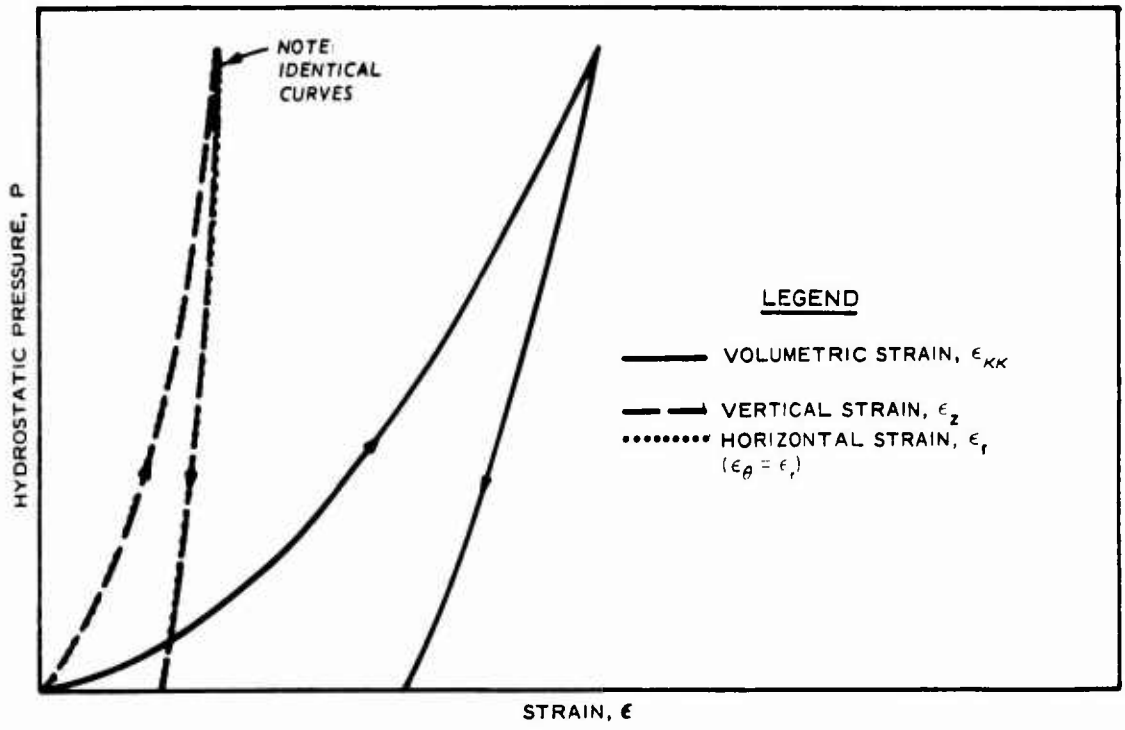

Figure 1. Typical behavior of a dry or undrained isotropic soil under hydrostatic loading and unloading

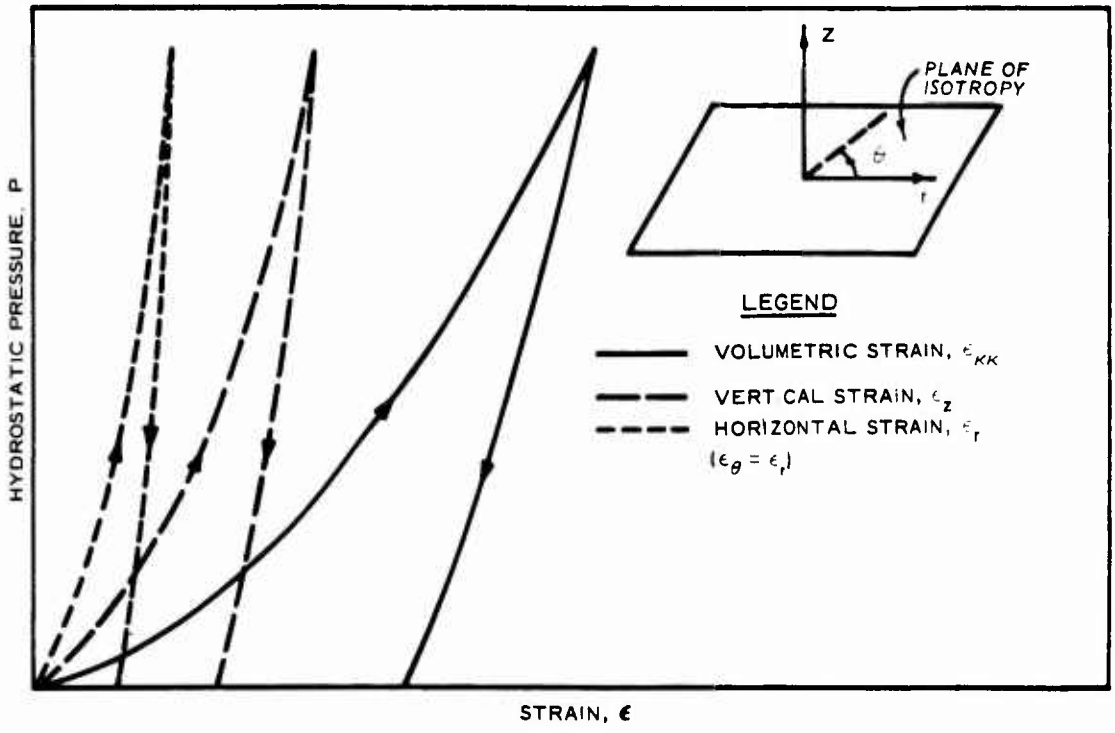

Figure 2. Typical behavior of a dry or drained transverse-isotropic soil under hydrostatic loading and unloading

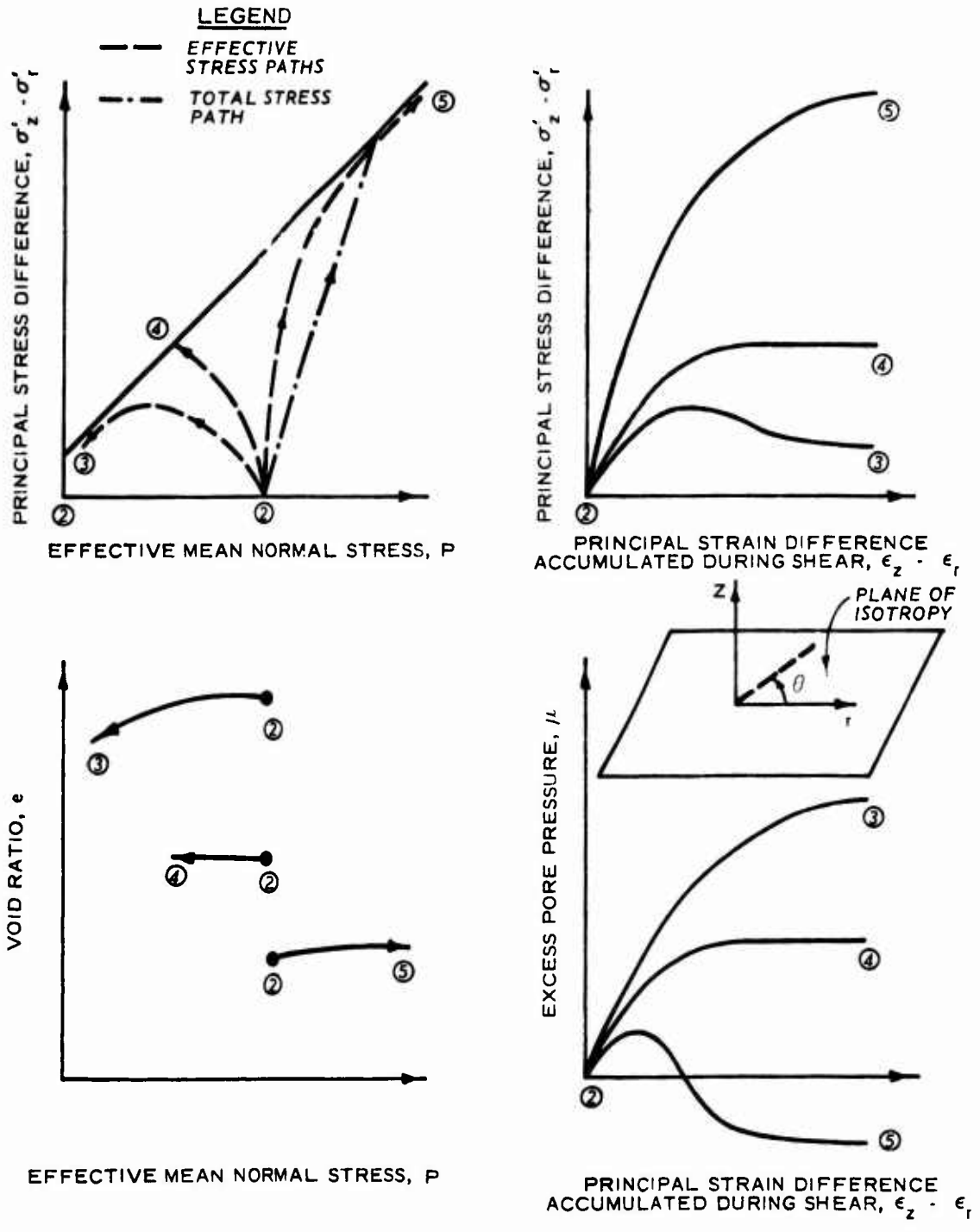

Figure 3. Typical behavior of saturated anisotropic soil tested under undrained triaxial test conditions

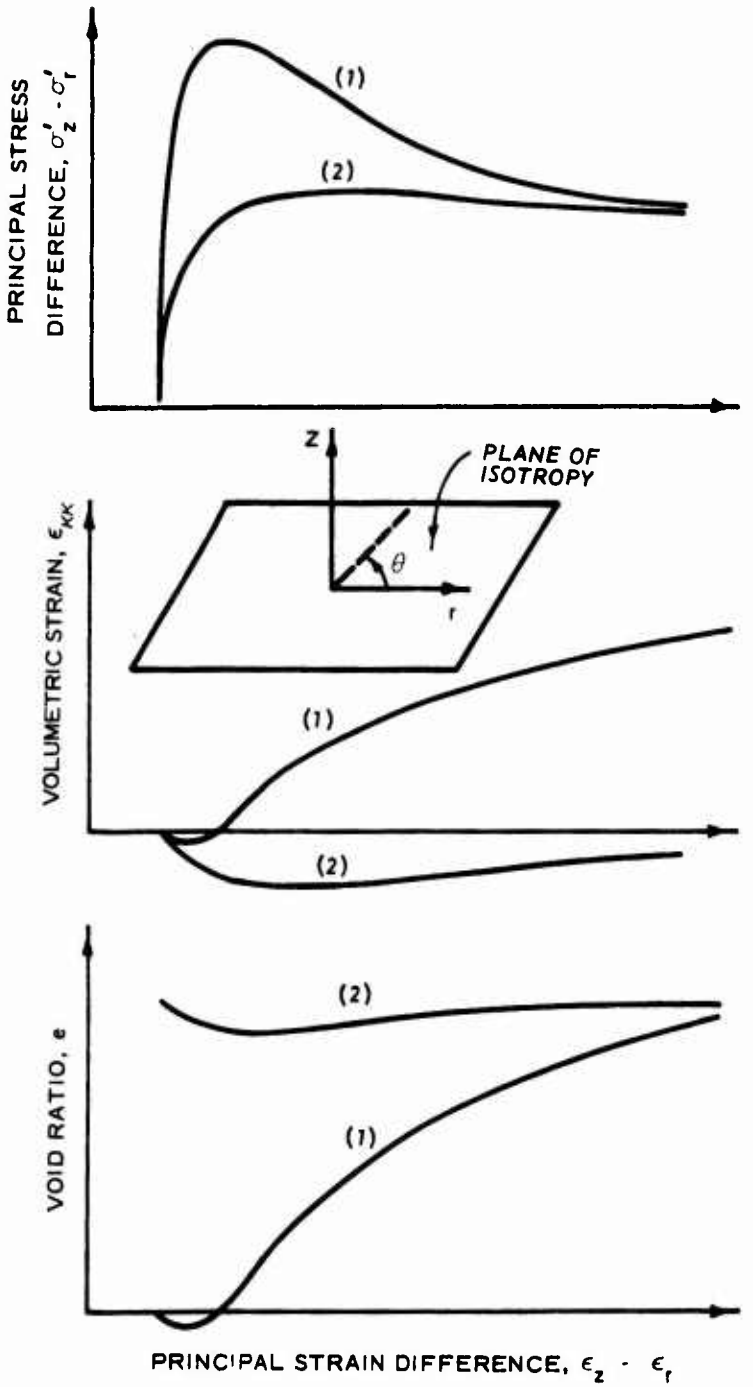

Figure 4. Typical mechanical response curves obtained for anisotropic soil specimens from drained triaxial tests: (1) overconsolidated clay or dense sand and (2) normally consolidated clay or loose sand

typical of loose sand or normally consolidated clay.

13. The mathematical development of a total stress (single-phase) elastic-plastic transverse-isotropic constitutive relationship that qualitatively describes the responses shown in Figures 1 through 4 is presented in Part III. The treatment of a multiphase system is presented in Part IV.

PART III: ELASTIC-PLASTIC CONSTITUTIVE MODEL

14. The fundamental relationships for linear elastic and elastic-plastic transverse-isotropic constitutive models are derived in Appendixes B and C, respectively. In this part, the most important mathematical expressions developed for the generalized model in these appendixes are utilized, but the focus is on specific forms of the model's response functions. For example, the definitions of the elastic and plastic pseudo stress invariants as given by Equations B13 and C14, respectively, and the elastic and plastic pseudo strain deviation increment tensors as given by Equations C11 and C22, respectively, are required. In addition, the general elastic description of the model as defined by Equations C6 through C12 and the general plastic description given by Equations C13 through C37 are needed. The model's complete generalized elastic-plastic description is governed by Equation C40. The above-cited equations are used to describe selected mathematical forms of the various response functions contained in the model, which are needed to simulate the typical soil responses presented in the previous sections.

Elastic Behavior

15. The behavior of the model in the elastic (recoverable) range is governed by the three constants, α^E, β^E, and γ^E, (Equation B13 of Appendix B) and by the two response functions, B and S, Equation C9 of Appendix C. Equation C10 reveals that the parameter α^E and the response function B are compressibility-related material properties, while Equation C11 reveals that the parameters β^E and γ^E and the response function S are shear-related material properties.

Compressibility-related material properties

16. The parameter α^E defines the ratio between the elastic strain in the plane of isotropy, ε_r, and the elastic strain normal to the plane of isotropy, ε_z, under hydrostatic states of stress (Figure 2); thus

$$\alpha^E = \frac{\varepsilon_r^E}{\varepsilon_z^E} \tag{5}$$

For the ensuing developments, it will be more convenient to work with a Cartesian coordinate system. Hence, the plane 22, 33 of the Cartesian coordinate system 11, 22, and 33 is designated as the plane of isotropy (Figure 5). Equation 5, therefore, becomes

$$\alpha^E = \frac{\varepsilon_{22}^E}{\varepsilon_{11}^E} = \frac{\varepsilon_{33}^E}{\varepsilon_{11}^E} \tag{6}$$

The value of α^E can be determined experimentally from the slope of the unloading strain path curve obtained from a hydrostatic compression test (Figure 5). It is clear from Figure 5 that for an isotropic material, the value of α^E becomes

$$\alpha^E = \frac{\varepsilon_{22}^E}{\varepsilon_{11}^E} = \frac{\varepsilon_{33}^E}{\varepsilon_{11}^E} = 1 \tag{7}$$

The elastic response function B (B is the elastic bulk modulus for an isotropic material) describes the unloading stress-strain response of a hydrostatic compression test (Figure 2). It is suggested that for most transverse-isotropic earth materials, B can be taken as a function of the first (elastic) pseudo invariant of stress ϕ_1^E, (Figure 6)*

$$B = \frac{B_i}{1 - B_1}\left[1 - B_1 \exp\left(- B_2 \phi_1^E\right)\right] \tag{8}$$

where

B_i = initial value of the response function B (Figure 6)

---

* The functional form of B can readily include more terms, thereby providing more flexibility in fitting the behavior of a specific material. The function B could also be dependent on the plastic volumetric strain.

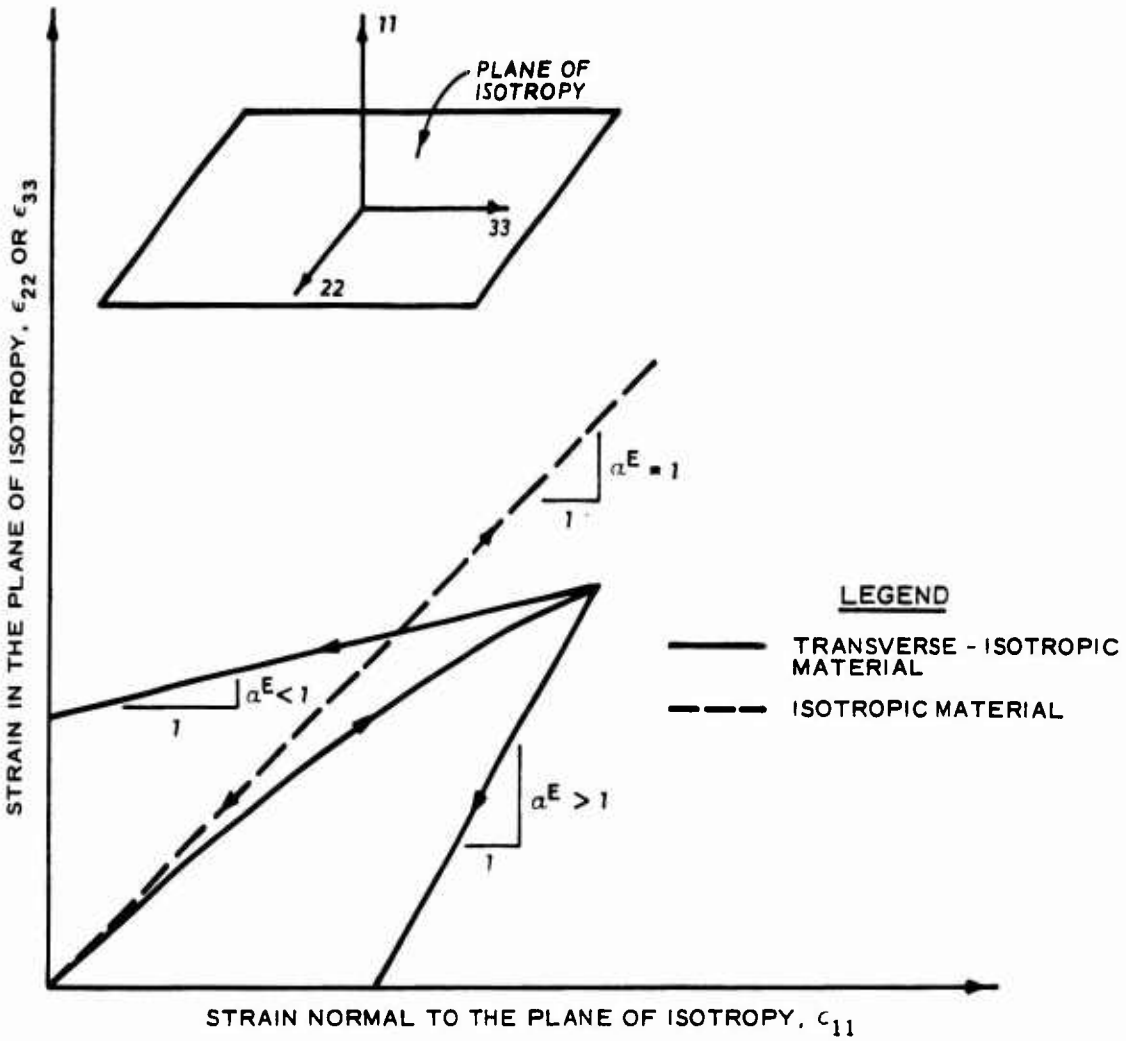

Figure 5. Comparison of strain paths for isotropic and transverse-isotropic materials subjected to hydrostatic loading and unloading

B_1, B_2 = material constants

Equation 8 above together with Equation C10 of Appendix C indicate that the material constants B_i, B_1, and B_2 can be readily determined experimentally from the unloading hydrostatic compression test results, as illustrated in Figure 7. Equation 8, therefore, can be written as

$$B = \frac{B_i}{1 - B_1}\left[1 - B_1 \exp\left(- B_2 \phi_1^E\right)\right] = \frac{d\phi_1^E}{9d\epsilon_{11}^E} \qquad (9)$$

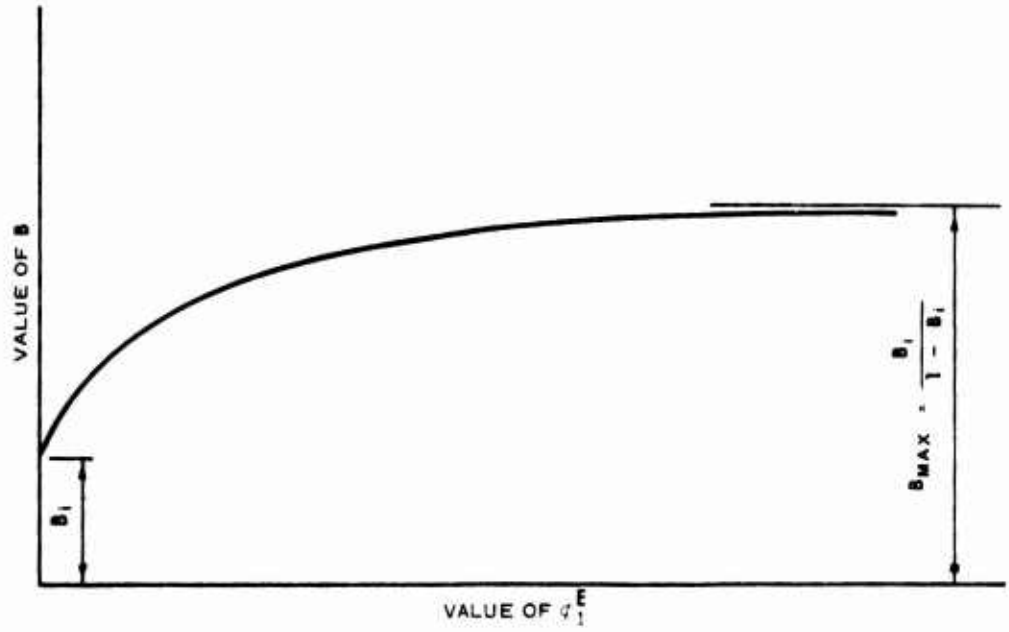

Figure 6. Elastic response function B versus first elastic pseudo invariant of stress ϕ_1^E

Shear-related material properties

17. The elastic shear response function S (S is the elastic shear modulus for an isotropic material) accounts for the curvature observed in the stress difference-strain difference results obtained from triaxial compression tests, (Figure 3). For this report, S is assumed to be a function of the second (elastic) pseudo invariant of stress ϕ_2^E, as well as the plastic volumetric strain, ε_{kk}^P, (Figure 8)*

$$S = \frac{S_i}{1 - S_1}\left[1 - S_1 \exp\left(-S_2\sqrt{\phi_2^E}\right)\right] + S_3\left[1 - \exp\left(-S_4\,\varepsilon_{kk}^P\right)\right] \qquad (10)$$

where

S_i = initial value of the response function S (Figure 8)

S_1, S_2, S_3, S_4 = material constants

* This functional form of S could include more terms, thereby providing for more flexibility in fitting the behavior of a specific material.

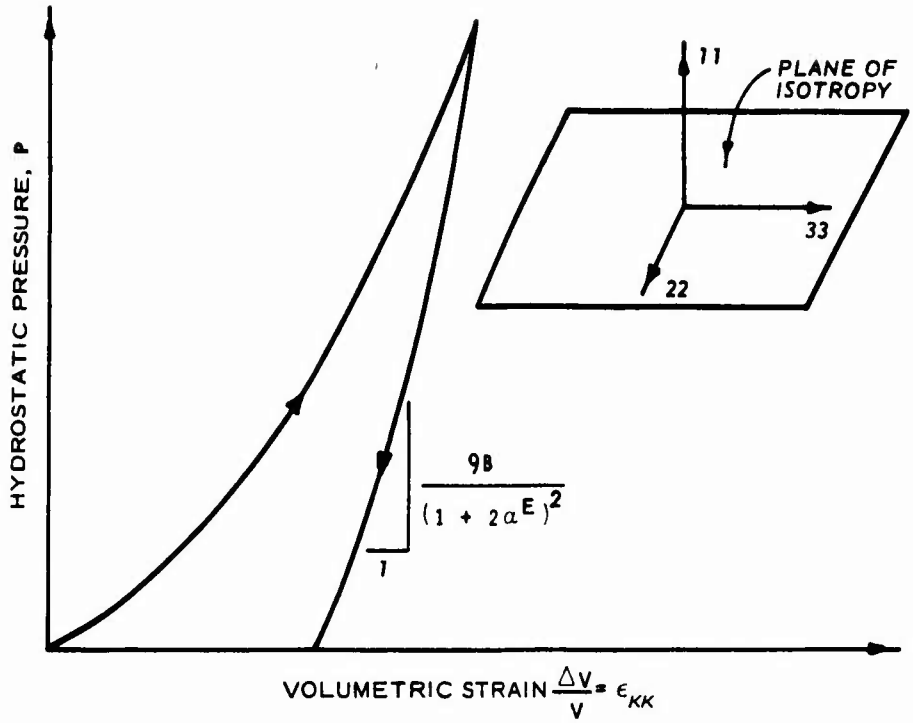

a. HYDROSTATIC COMPRESSION

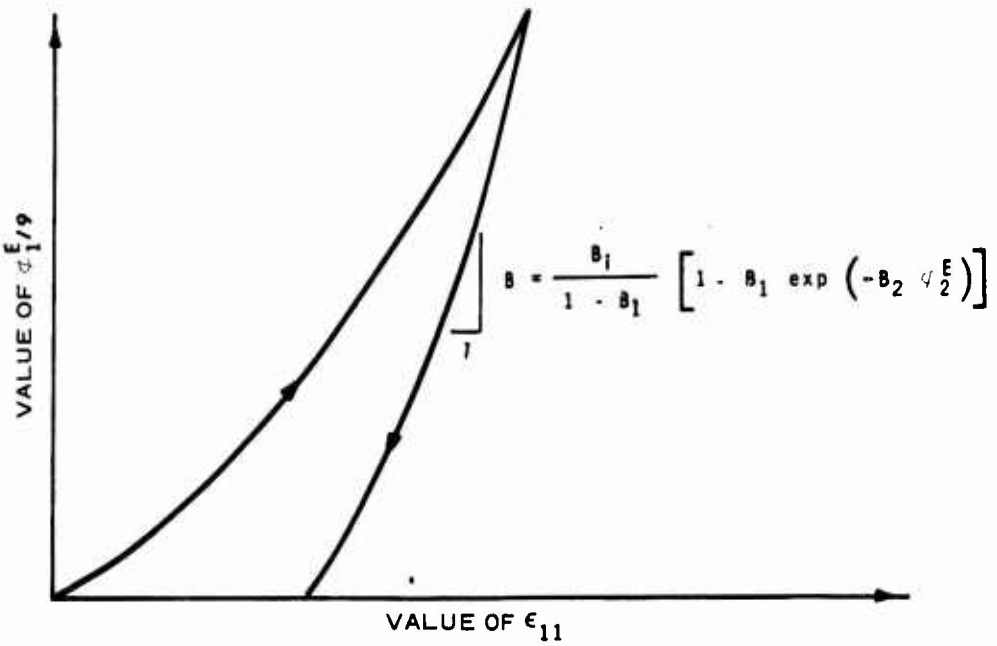

b. METHOD FOR ISOLATING RESPONSE FUNCTION B

Figure 7. Elastic transverse-isotropic relationships for hydrostatic compression test

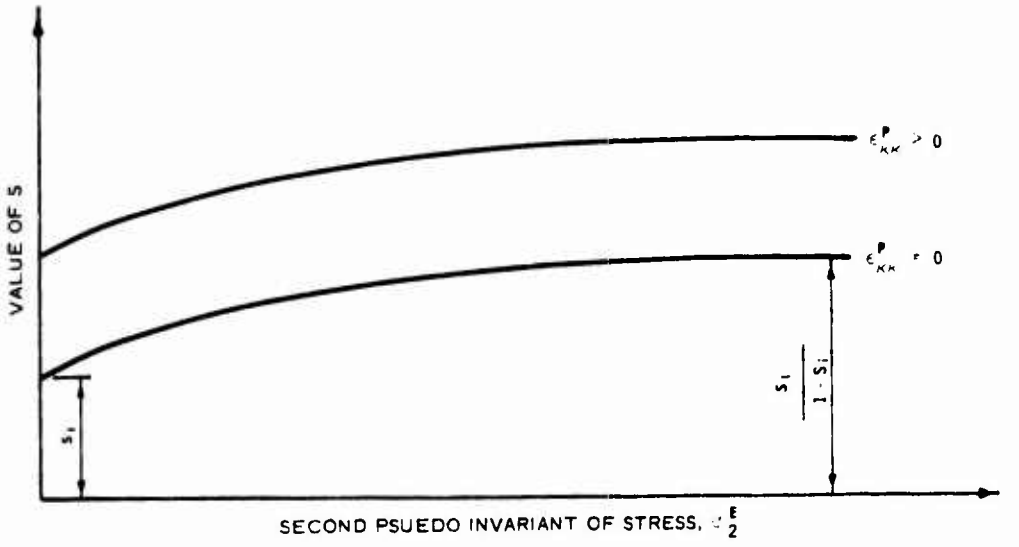

Figure 8. Elastic response function S versus second pseudo invariant of stress and the plastic volumetric strain

Equation C11 of Appendix C indicates that the material constants S_i, S_1, S_2, S_3, and S_4 can be readily determined from the slopes of experimental unloading stress-strain curves obtained from a series of triaxial tests conducted on a cubical specimen, i.e., a 3-D box type test, at different confining pressures in which the axial stress is applied paralled to the 33-axis, i.e., $\sigma_{11} = \sigma_{22}$ = confining pressure (Figure 9). The results of these same tests can be used to determine the value of β^E from the slope of the unloading strain path shown in Figure 10:

$$\beta^E = \frac{\bar{e}^E_{11}}{\bar{e}^E_{22}} \tag{11}$$

where $\bar{e}^E_{ij}$ is the elastic pseudo strain deviation tensor defined by Equations C11 and C12 of Appendix C. There are several ways of determining γ^E. One way is to measure the unloading shear stress-shear strain response during a direct shear test, or a simple shear test, (Figure 11). The slope of the $\sigma_{13} - \epsilon_{13}$ unloading curve is equal to $2S/\gamma^E$, from which γ^E can be easily determined, since the function S is known from Figures 8 and 9.

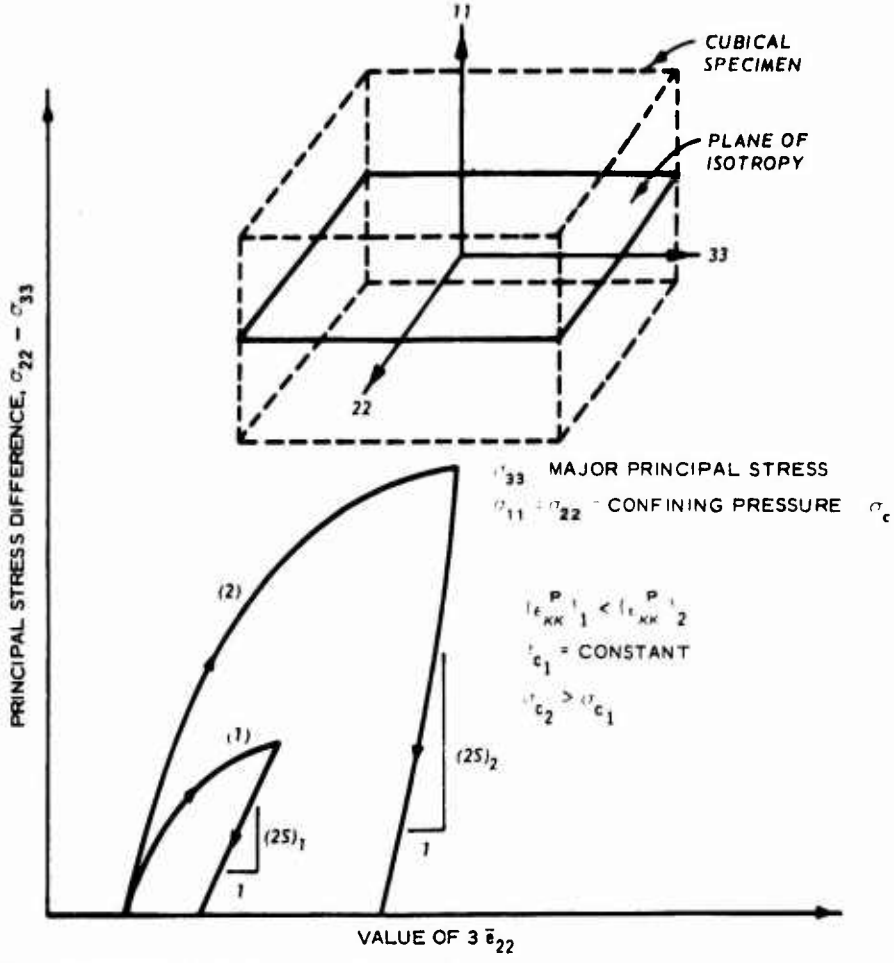

Figure 9. Suggested method for conducting triaxial tests and plotting results to quantitatively determine the response function S

Plastic Behavior

18. For the plastic behavior, the loading function f (Equation C13 of Appendix C) is assumed to consist of two parts (Figure 12): an ultimate failure envelope that effectively limits the maximum shear stress in the material and an elliptically-shaped strain-hardening yield surface that produces plastic volumetric and shear strains as it moves. The failure envelope portion of the loading function is mathematically described by

$$f\left(\phi_1^P, \sqrt{\phi_2^P}\right) = \sqrt{\phi_2^P} - \psi\, \phi_1^P - k \qquad (12)$$

and the strain-hardening yield surface by

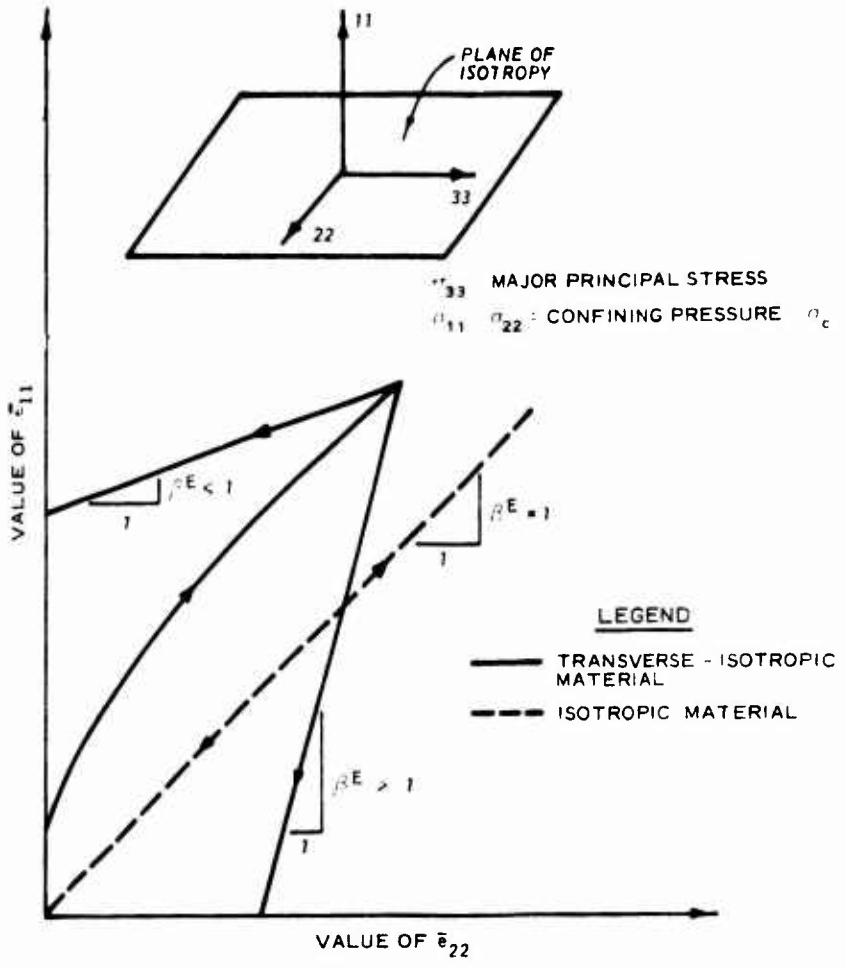

Figure 10. Comparison of lateral strain path results for isotropic and transverse-isotropic materials subjected to a triaxial test

$$F\left(\phi_1^P, \sqrt{\phi_2^P}, \kappa\right) = \left[\phi_1^P - L(\kappa)\right]^2 + R^2\phi_2^P - \left[X(\kappa) - L(\kappa)\right]^2 = 0 \quad (13)$$

where ϕ_1^P and ϕ_2^P are, respectively, the first and second (plastic) pseudo invariants of stress, which are defined by Equation C14 of Appendix C; and parameters k and ψ are material constants representing pseudo cohesive and frictional strength parameters of the material (Figure 12); R is a parameter which will be defined below; $X(\kappa)$ and $L(\kappa)$ define the intersections of the hardening surface with the ϕ_1^P axis and the failure envelope $f\left(\phi_1^P, \sqrt{\phi_2^P}\right)$, respectively; and κ is the hardening parameter, which generally is a function of the

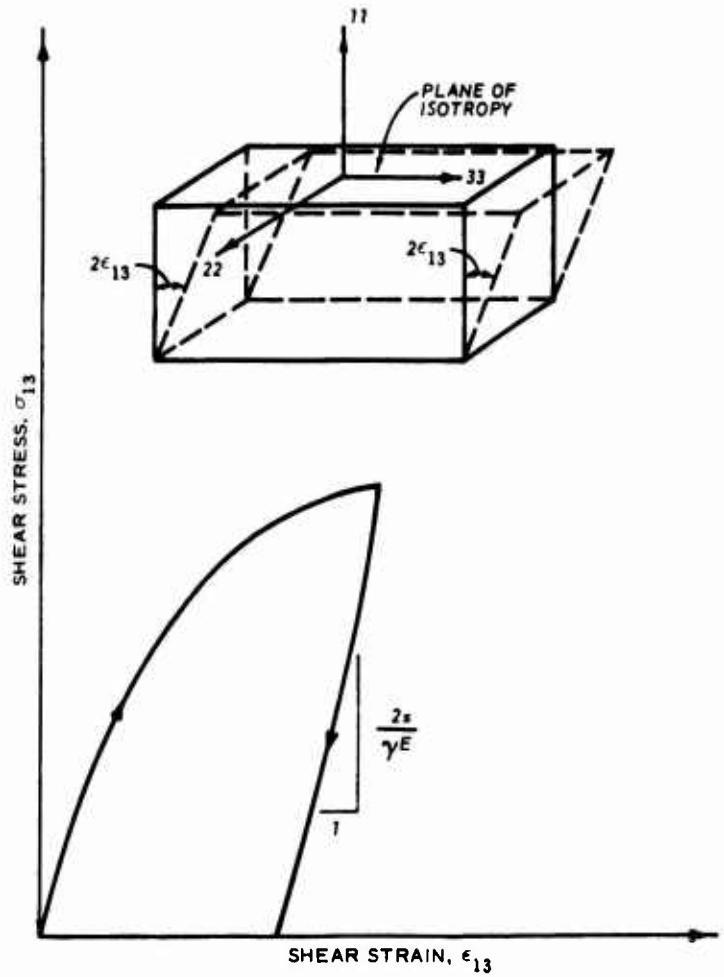

Figure 11. Simple shearing stress-strain response of a transverse-isotropic material

history of plastic volumetric strain, ε_{kk}^P. For most soils, κ can be chosen as

$$\kappa = \varepsilon_{kk}^P \tag{14}$$

Equation 14 allows for the elliptic hardening surface to expand and contract as well as to translate relative to the origin of the ϕ_1^P, $\sqrt{\phi_2^P}$ axes. Note that the hardening surface (Figure 12) was chosen so

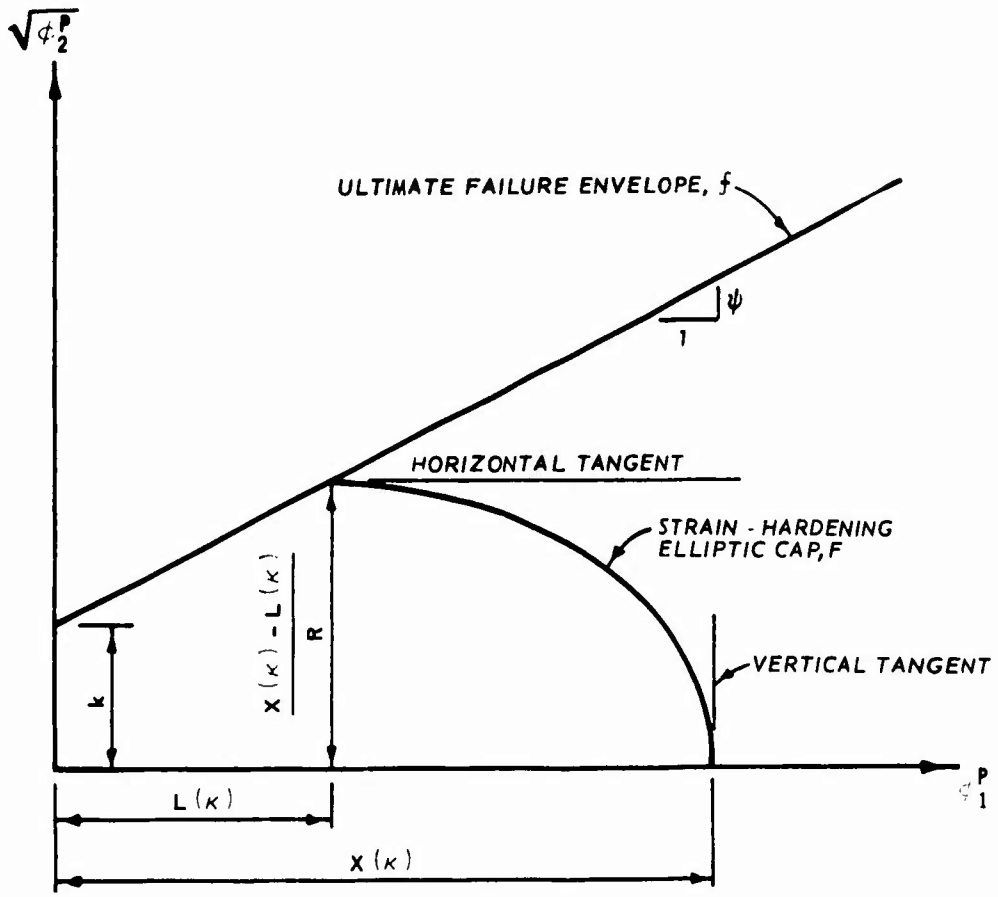

Figure 12. Proposed yield surface for the elastic-plastic transverse-isotropic model

that the tangent at its intersection with the failure envelope is horizontal. This condition is guaranteed by the following relationships between κ , $L(\kappa)$, and $X(\kappa)$:*

$$L(\kappa) = \begin{cases} \ell(\kappa) & \text{if } \ell(\kappa) > 0 \\ 0 & \text{if } \ell(\kappa) \leq 0 \end{cases} \tag{15}$$

---

* The mathematical form of Equation 16 depends on the specific material being modeled. The author believes, however, that the form presented by Equation 16 is suitable for modeling most soils when subjected to a relatively low stress level.

$$X(\kappa) = -\frac{1}{D} \ln \left(1 - \frac{\kappa}{W}\right) \tag{16}$$

$$\ell(\kappa) = \frac{X(\kappa) - Rk}{1 + \psi R} = \frac{-\frac{1}{D} \ln \left(1 - \frac{\kappa}{W}\right) - Rk}{1 + \psi R} \tag{17}$$

where D is a material constant and W is also a material constant which defines the maximum plastic volumetric compaction that the material can experience under hydrostatic loading (Figure 13). The material parameter, R, in Equations 13 and 17, is the ratio of the major to the minor axes of the elliptic yield surface (Figure 12). The value

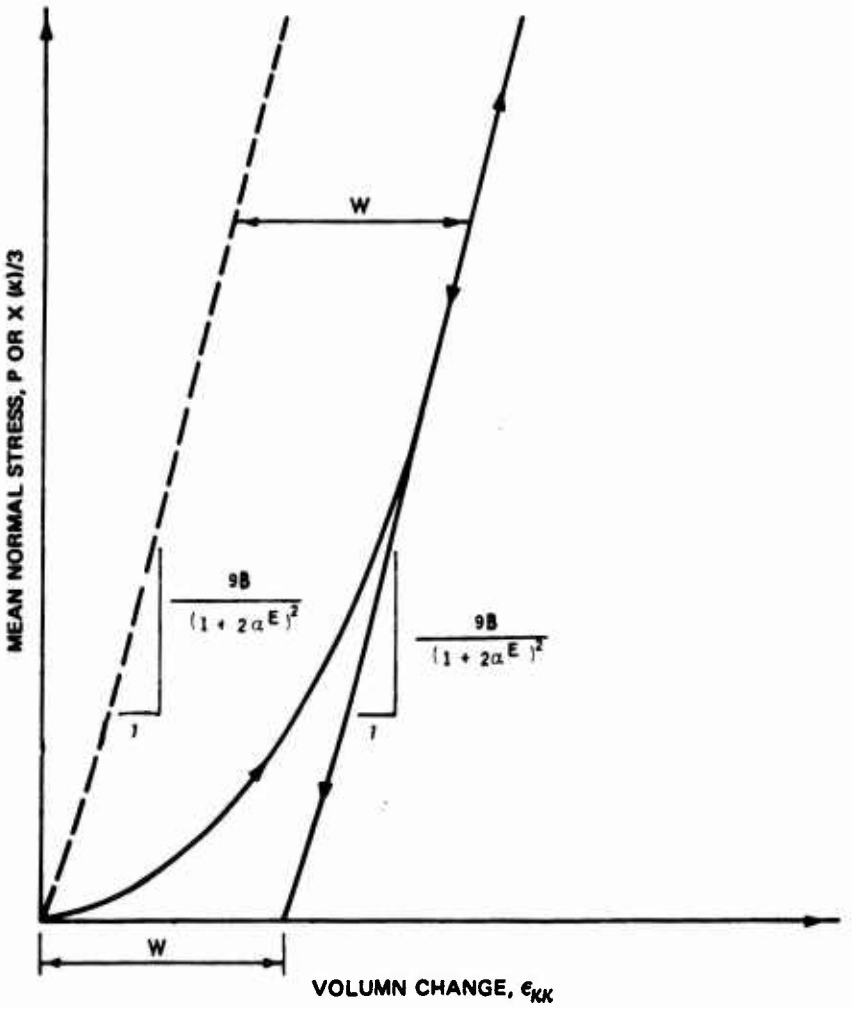

Figure 13. Behavior of model under hydrostatic compression, illustrating maximum irreversible volume change

of R depends on the state of compaction of the material. For a contractive material (i.e., loose sand or normally consolidated clay, Figure 3 curves marked "2 → 3"), the value of R is greater than $1/\psi$, whereas for a dilative material (i.e., dense sand or overconsolidated clay, Figure 3 curves marked "2 → 5"), the value of R is less than $1/\psi$. $R = 1/\psi$ corresponds to the curves marked "2 → 4" in Figure 3. These variations in the parameter R can be accounted for by the following relation:

$$R = \frac{R_i}{1 + R_1} \left\{ 1 + R_1 \exp \left[- R_2 L(\kappa) \right] \right\} \tag{18}$$

where R_i, R_1, and R_2 are material constants that can be determined by a trial and error process of fitting the model to a variety of laboratory test data.

19. The material parameters ψ and k (Figures 12 and 14, and Equation 12) can be determined from a series of standard triaxial tests in which the material is sheared to failure. The material parameters α^P and β^P appearing in the definitions of ϕ_1^P and ϕ_2^P are defined analogously to their elastic counterparts, except that they involve the plastic strains instead of the elastic strains, i.e., (see Figures 5 and 10, and Equations 6 and 11):

$$\alpha^P = \frac{\varepsilon_{22}^P}{\varepsilon_{11}^P} = \frac{\varepsilon_{33}^P}{\varepsilon_{11}^P} \tag{19}$$

$$\beta^P = \frac{\bar{e}_{11}^P}{\bar{e}_{22}^P} \tag{20}$$

where $\bar{e}_{ij}^P$ is the pseudo plastic strain deviation tensor that is defined by Equations C22 and C23 of Appendix C. The parameter γ^P cannot be expressed analogously to its elastic counterpart (Figure 11),

because it involves the plastic stress-strain relation,[15] i.e.,

$$\gamma^P = \frac{d\varepsilon_{21}^P}{\frac{d\lambda}{2\sqrt{\phi_2^P}} \frac{\partial f}{\partial \sqrt{\phi_2^P}} \sigma_{21}} \tag{21}$$

The parameters α^P and β^P affect the shape of the failure and hardening yield surfaces. This can be seen most clearly in principal stress space (Figure 14). In the octahedral plane, the trace of the

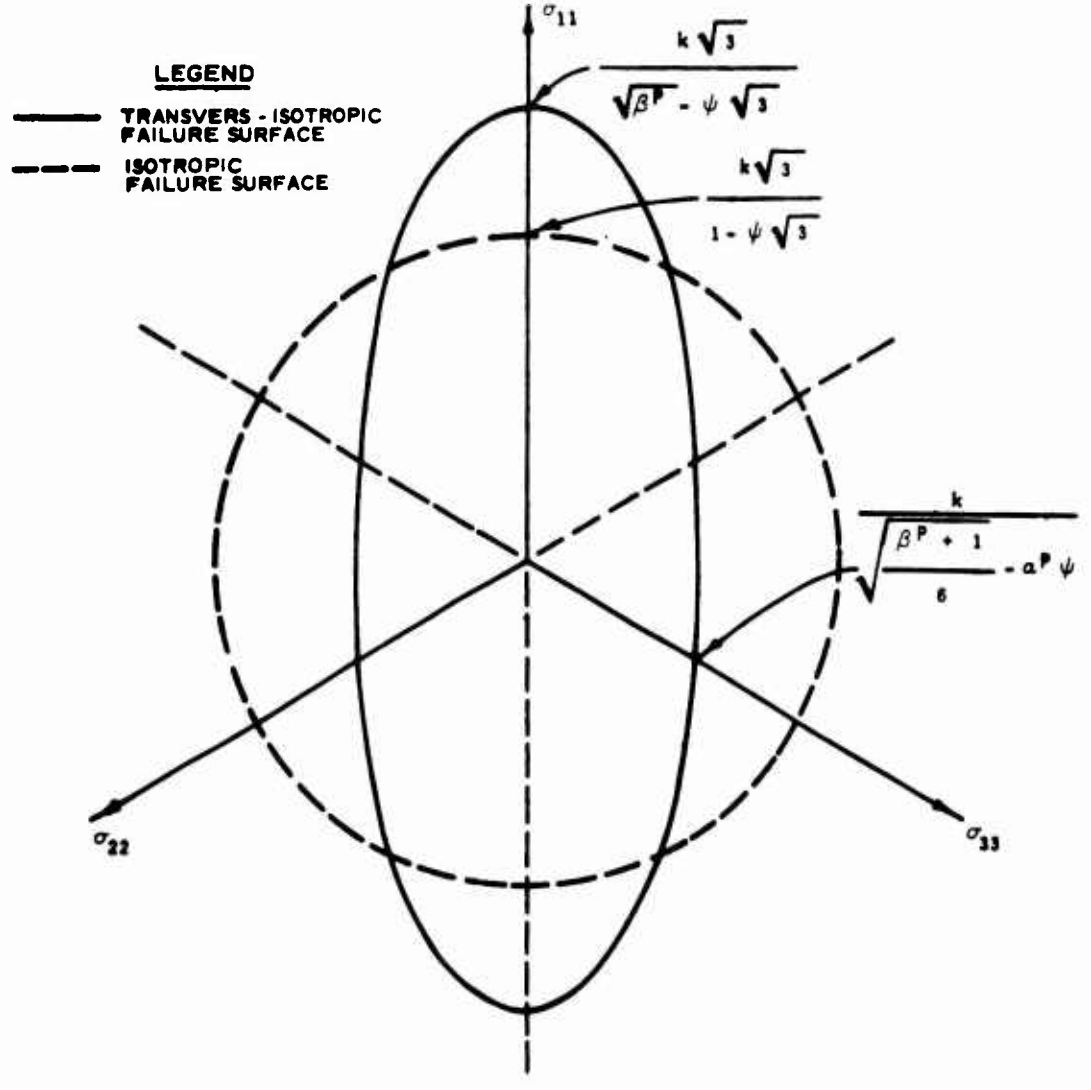

Figure 14. Isotropic and transverse-isotropic failure surfaces in octahedral plane

failure surface defined by Equation 12 is shaped like an ellipse (Figure 14). The dashed circle in Figure 14 represents the trace of a failure surface for which $\alpha^P = \beta^P = 1$.

20. In summary, there are five potential functions (two elastic, three plastic) and six material parameters (the α's , β's and γ's) that describe the complete behavior of the proposed model. These are summarized in Table 1. Twenty-one material constants are used in the present model. The treatment of a multiphase system using the proposed model is presented in Part IV.

PART IV: THE TREATMENT OF A MULTIPHASE SYSTEM

21. To model the behavior of a multiphase system, two separate sets of material constants, such as those shown in Table 1 are required. The first set should reflect the effective stress properties, i.e., those of the soil skeleton along, and should be determined by testing the material under drained conditions. The second set should reflect the total stress properties, i.e., those of the soil skeleton and water and air mixture, which should be determined by testing the material under undrained conditions. The resulting two sets of model parameters are summarized in Table 2. By use of these two sets of parameters, the complete pore pressure and total and effective stress response of a multi-phase system subjected to given stress or strain increments can be readily calculated by one of the following procedures:

a. If stress increments are given,

   1. Calculate the undrained volumetric strain using the second set of response functions and material constants listed in Table 2.

   2. Impose the above volume change on the drained model (i.e., the first set of response functions and material constants listed in Table 2) and calculate the resulting stress path and associated material response. This stress path is the effective stress path that the material will experience during this undrained load application. The pore pressure is simply the difference between the total and the effective stress paths.

   This procedure is illustrated in the diagram on page 28.

b. If strain increments are given,

   1. Calculate effective stresses using the first (drained) set of response functions and material constants listed in Table 2.

   2. Calculate total stresses using the second set of response functions and material constants listed in Table 2. The pore pressure during this undrained load application is simply the difference between the total and effective normal stresses.

   The diagram on page 29 illustrates this procedure.

The response of a multiphase material tested under undrained standard triaxial test conditions is calculated using one of the above-mentioned procedures in Part V.

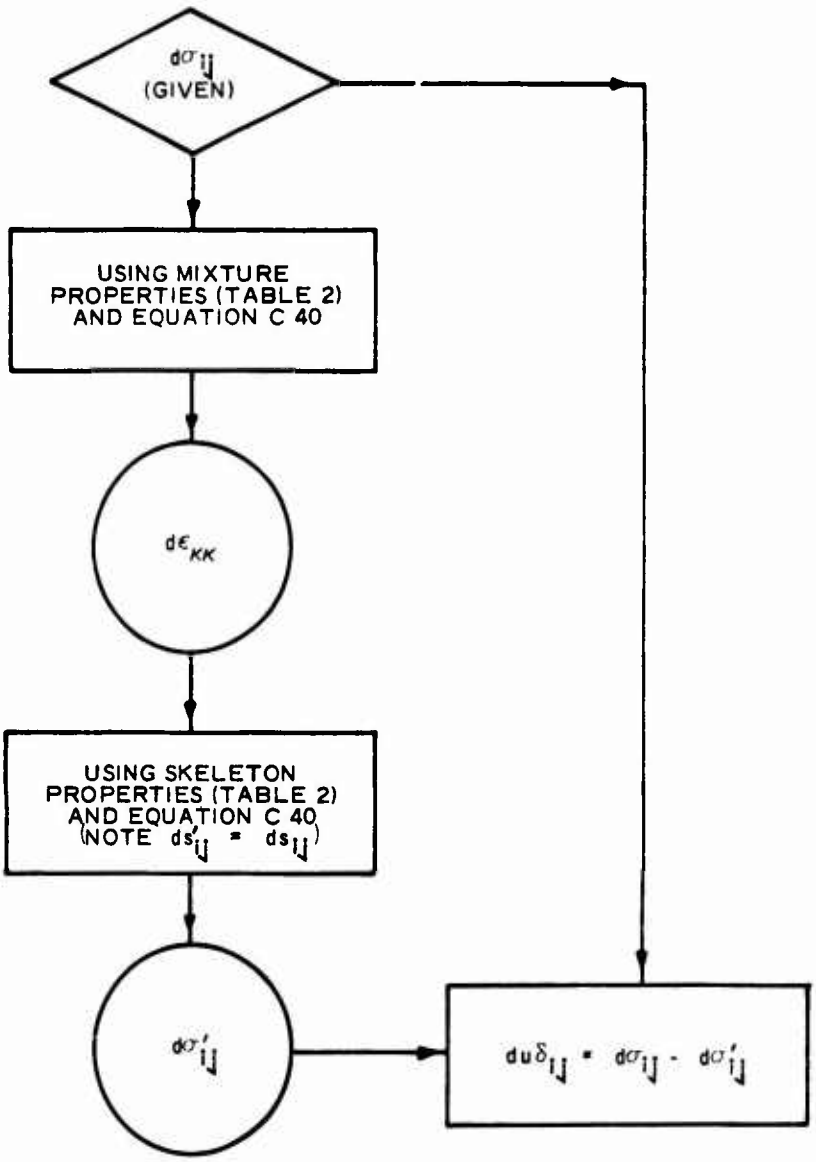

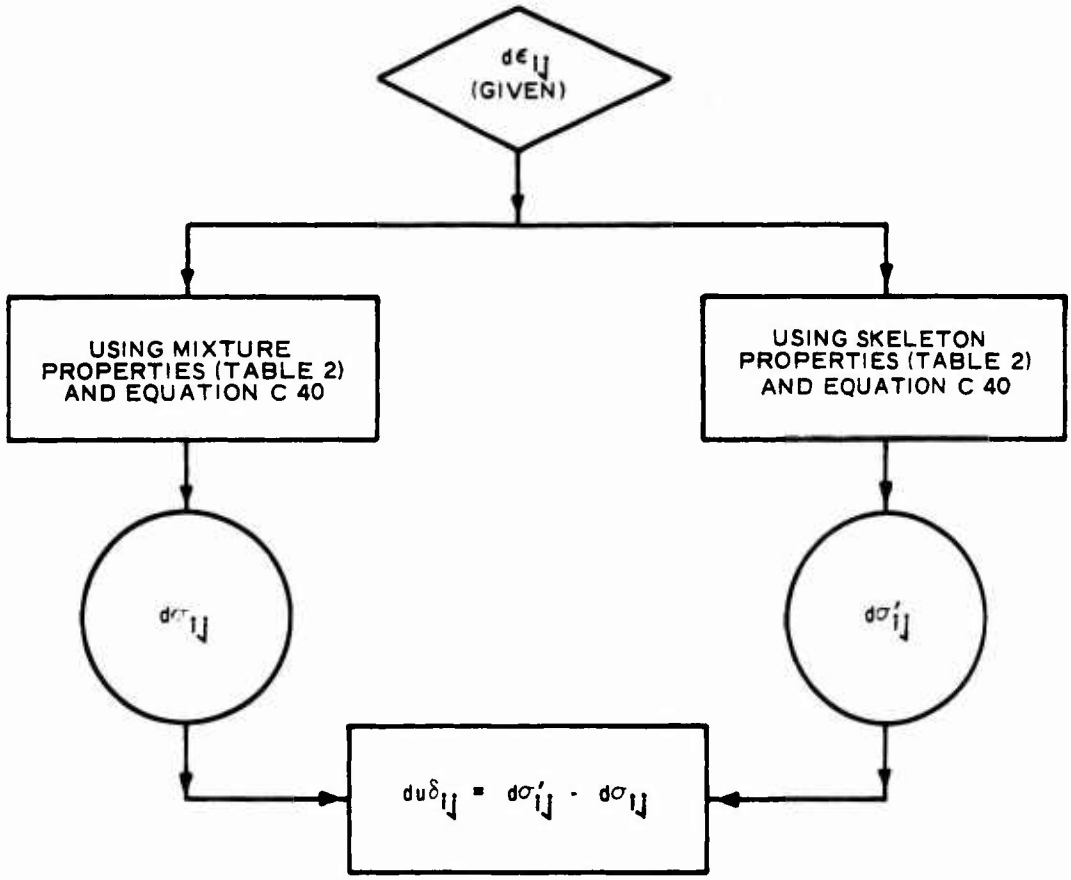
$d\epsilon_{ij}$
(GIVEN)
USING MIXTURE PROPERTIES (TABLE 2) AND EQUATION C 40
USING SKELETON PROPERTIES (TABLE 2) AND EQUATION C 40
$d\sigma_{ij}$
$d\sigma'_{ij}$
$du\delta_{ij} = d\sigma'_{ij} - d\sigma_{ij}$

PART V: BEHAVIOR OF THE MULTIPHASE CONSTITUTIVE MODEL UNDER TRIAXIAL TEST CONDITIONS

22. The ability of the model to simulate the response of a multiphase system can be more clearly understood if the model is examined under particular laboratory test boundary conditions. Since most of the mechanical testing of soils for engineering purposes is performed with the triaxial test (TX) apparatus, it is appropriate to investigate the model under both drained and undrained TX conditions. Adopting the z-axis of a cylindrical coordinate system (z , r , and θ) as the axis of symmetry of both the material and the soil sample (i.e., the plane $r\theta$ is the plane of isotropy of the material), the total and effective stress tensors, and the strain tensor associated with this configuration become:

$$\sigma_{ij} = \begin{bmatrix} \sigma_z & 0 & 0 \\ 0 & \sigma_r & 0 \\ 0 & 0 & \sigma_r \end{bmatrix} \tag{22}$$

$$\sigma'_{ij} = \begin{bmatrix} \sigma'_z & 0 & 0 \\ 0 & \sigma'_r & 0 \\ 0 & 0 & \sigma'_r \end{bmatrix} \tag{23}$$

$$\varepsilon_{ij} = \begin{bmatrix} \varepsilon_z & 0 & 0 \\ 0 & \varepsilon_r & 0 \\ 0 & 0 & \varepsilon_r \end{bmatrix} \tag{24}$$

The variables J_1 , J'_1 , $\bar{J}_2$, $\bar{J}'_2$, ϕ_1^E , $\phi_1'^E$, ϕ_1^P , $\phi_1'^P$, ϕ_2^E , $\phi_2'^E$, ϕ_2^P , $\phi_2'^P$, and ε_{kk} associated with the above-mentioned stress and strain tensors take the following forms:

$$J_1 = \sigma_z + 2\sigma_r \tag{25}$$

$$J_1' = \sigma_z' + 2\sigma_r' \tag{26}$$

$$\bar{J}_2 = \bar{J}_2' = \frac{1}{3}(\sigma_z - \sigma_r)^2 = \frac{1}{3}(\sigma_z' - \sigma_r')^2 \tag{27}$$

$$\phi_1^E = \sigma_z + 2\alpha_m^E \sigma_r \tag{28}$$

$$\phi_1'^E = \sigma_z' + 2\alpha_s^E \sigma_r' \tag{29}$$

$$\phi_1^P = \sigma_z + 2\alpha_m^P \sigma_r \tag{30}$$

$$\phi_1'^P = \sigma_z' + 2\alpha_s^P \sigma_r' \tag{31}$$

$$\phi_2^E = \frac{\beta_m^E}{3}(\sigma_z - \sigma_r)^2 \tag{32}$$

$$\phi_2'^E = \frac{\beta_s^E}{3}(\sigma_z' - \sigma_r')^2 \tag{33}$$

$$\phi_2^P = \frac{\beta_m^P}{3}(\sigma_z - \sigma_r)^2 \tag{34}$$

$$\phi_2'^P = \frac{\beta_s^P}{3}(\sigma_z' - \sigma_r')^2 \tag{35}$$

$$\varepsilon_{kk} = \varepsilon_z + 2\varepsilon_r \tag{36}$$

where

J_1 = first invariant of the total stress tensor

J_1' = first invariant of the effective stress tensor

$\bar{J}_2 = \bar{J}_2'$ = second invariant of the total or effective stress deviation tensor

ϕ_1^E = elastic first pseudo invariant of total stress

$\phi_1'^E$ = elastic first pseudo invariant of effective stress

ϕ_1^P = plastic first pseudo invariant of total stress

$\phi_1'^P$ = plastic first pseudo invariant of effective stress

ϕ_2^E = elastic second pseudo invariant of total stress

$\phi_2'^E$ = elastic second pseudo invariant of effective stress

ϕ_2^P = plastic second pseudo invariant of total stress

$\phi_2'^P$ = plastic second pseudo invariant of effective stress

ε_{kk} = volumetric strain

The triaxial test generally has two phases: the hydrostatic phase and the shear phase. Both phases can be conducted either drained or undrained. These phases are discussed below.

Hydrostatic Phase

Drained condition

23. During the drained hydrostatic phase of a triaxial test, the pore pressure is zero and

$$\sigma_z' = \sigma_r' = \sigma_\theta' \tag{37}$$

$$\varepsilon_{kk} = \varepsilon_z + 2\varepsilon_r \tag{38}$$

where $\varepsilon_\theta = \varepsilon_r$. The relation between the elastic volumetric strain increment and the increment of the first pseudo invariant of effective stress is given as (see Equation C10 of Appendix C and Table 2)

$$d\phi_1'^E = \frac{9B_s}{1 + 2\alpha_s^E} d\varepsilon_{kk}^E \tag{39}$$

where the response function B_s is given by Equation 8 or 9. Equation 8 is substituted into Equation 39 and the resulting expression is

integrated to provide the following relation between the elastic volumetric strain ε_{kk}^{E} and $\phi_1'^{E}$:

$$\varepsilon_{kk}^{E} = \left(\frac{1 + 2\alpha_s^E}{9}\right)\left(\frac{1 - B_{1s}}{B_{2s}\ B_{is}}\right) \ln\left[\frac{\exp\left(B_{2s}\ \phi_1'^{E}\right) - B_{1s}}{1 - B_{1s}}\right] \tag{40}$$

In view of Equation 5, the elastic radial and vertical strains can be written as

$$\varepsilon_r^E = \frac{\alpha_s^E}{9}\left(\frac{1 - B_{1s}}{B_{2s}\ B_{is}}\right) \ln\left[\frac{\exp\left(B_{2s}\ \phi_1'^{E}\right) - B_{1s}}{1 - B_{1s}}\right] \tag{41}$$

and

$$\varepsilon_z^E = \frac{1}{9}\left(\frac{1 - B_{1s}}{B_{2s}\ B_{is}}\right) \ln\left[\frac{\exp\left(B_{2s}\ \phi_1'^{E}\right) - B_{1s}}{1 - B_{1s}}\right] \tag{42}$$

The relation between the plastic volumetric strain, ε_{kk}^{P}, and $\phi_1'^{P}$ is given by Equation 16, where κ for this phase of the test is ε_{kk}^{P} and $X(\kappa)$ is $\phi_1'^{P}$, thus:

$$\varepsilon_{kk}^{P} = W_s\left[1 - \exp\left(-D_s\ \phi_1'^{P}\right)\right] \tag{43}$$

By the use of Equations B13 and C14, the relationship between $\phi_1'^{E}$ and $\phi_1'^{P}$ under a hydrostatic state of stress is

$$\phi_1'^{P} = \left(\frac{1 + 2\alpha_s^P}{1 + 2\alpha_s^E}\right)\phi_1'^{E} \tag{44}$$

Substitution of Equation 44 into Equation 43 yields

$$\varepsilon_{kk}^{P} = W_s\left\{1 - \exp\left[-\left(1 + 2\alpha_s^P\right) D_s\ \phi_1'^{E} \Big/ \left(1 + 2\alpha_s^E\right)\right]\right\} \tag{45}$$

The plastic radial and vertical strains can be obtained by the combination of Equations 19 and 45:

$$\varepsilon_r^P = \left(\frac{W_s\ \alpha_s^P}{1 + 2\alpha_s^P}\right)\left\{1 - \exp\left[-\left(1 + 2\alpha_s^P\right) D_s\ \phi_1'^E \Big/ \left(1 + 2\alpha_s^E\right)\right]\right\} \quad (46)$$

and

$$\varepsilon_z^P = \left(\frac{W_s}{1 + 2\alpha_s^P}\right)\left\{1 - \exp\left[-\left(1 + 2\alpha_s^P\right) D_s\ \phi_1'^E \Big/ \left(1 + 2\alpha_s^E\right)\right]\right\} \quad (47)$$

The total (elastic plus plastic) strains can be easily obtained by the addition of Equations 41 and 46 for radial strain, Equations 42 and 47 for vertical strain, and Equations 40 and 45 for volumetric strain--which gives:

$$\varepsilon_r = \alpha_s^E \left(\frac{1 - B_{1s}}{9B_{2s}\ B_{is}}\right) \ln\left[\frac{\exp\left(B_{2s}\ \phi_1'^E\right) - B_{1s}}{1 - B_{1s}}\right] + \left(\frac{W_s\ \alpha_s^P}{1 + 2\alpha_s^P}\right)\left\{1 - \exp\left[-\left(1 + 2\alpha_s^P\right) D_s\ \phi_1'^E \Big/ \left(1 + 2\alpha_s^E\right)\right]\right\} \quad (48)$$

$$\varepsilon_z = \left(\frac{1 - B_{1s}}{9B_{2s}\ B_{is}}\right) \ln\left[\frac{\exp\left(B_{2s}\ \phi_1'^E\right) - B_{is}}{1 - B_{is}}\right] + \left(\frac{W_s}{1 + 2\alpha_s^P}\right)\left\{1 - \exp\left[-\left(1 + 2\alpha_s^P\right) D_s\ \phi_1'^E \Big/ \left(1 + 2\alpha_s^E\right)\right]\right\} \quad (49)$$

and

$$\varepsilon_{kk} = \left(1 + 2\alpha_s^E\right)\left(\frac{1 - B_{is}}{9B_{2s}\ B_{is}}\right) \ln\left[\frac{\exp\left(B_{2s}\ \phi_1'^E\right) - B_{1s}}{1 - B_{1s}}\right] + W_s\left\{1 - \exp\left[-\left(1 + 2\alpha_s^P\right) D_s\ \phi_1'^E \Big/ \left(1 + 2\alpha_s^E\right)\right]\right\} \quad (50)$$

Equations 39 through 50 provide a complete specification for the deformation response of the material subjected to a drained hydrostatic test (i.e., isotropic consolidation).

24. The qualitative behavior of the model during a drained hydrostatic test is shown in Figure 15. The slope of the $\phi_1'^E - \varepsilon_{kk}$ and $J_1' - \varepsilon_{kk}$ curves during virgin loading can be obtained from Equation 50:

$$\frac{d\phi_1'^E}{d\varepsilon_{kk}} = \frac{1}{d1 + d2} \tag{51}$$

where

$$d1 = \frac{1}{\frac{9B_{is}}{\left(1 + 2\alpha_s^E\right)\left(1 - B_{1s}\right)}\left[1 - B_{1s}\exp\left(-B_{2s}\,\phi_1'^E\right)\right]}$$

$$d2 = W_s D_s \left(\frac{1 + 2\alpha_s^P}{1 + 2\alpha_s^E}\right) \exp\left[-\left(1 + 2\alpha_s^P\right) D_s\,\phi_1'^E \Big/ \left(1 + 2\alpha_s^E\right)\right]$$

The combination of Equations 8, 45 and 51 results in:

$$\frac{d\phi_1'^E}{d\varepsilon_{kk}} = \frac{1}{\frac{1}{\left(\frac{9}{1 + 2\alpha_s^E}\right)B_s} + D_s\left(\frac{1 + 2\alpha_s^P}{1 + 2\alpha_s^E}\right)\left(W_s - \varepsilon_{kk}^P\right)} \tag{52}$$

The slope of the $J_1' - \varepsilon_{kk}$ curve can be easily obtained from Equation 52 by recognizing that the value of $\phi_1'^E$ for hydrostatic states of stress can be written as (see Equation B13 of Appendix B).

$$\phi_1'^E = \left(1 + 2\alpha_s^E\right)\sigma_z' = \left(1 + 2\alpha_s^E\right) J_1'/3 \tag{53}$$

Substitution of Equation 53 into Equation 52 leads to:

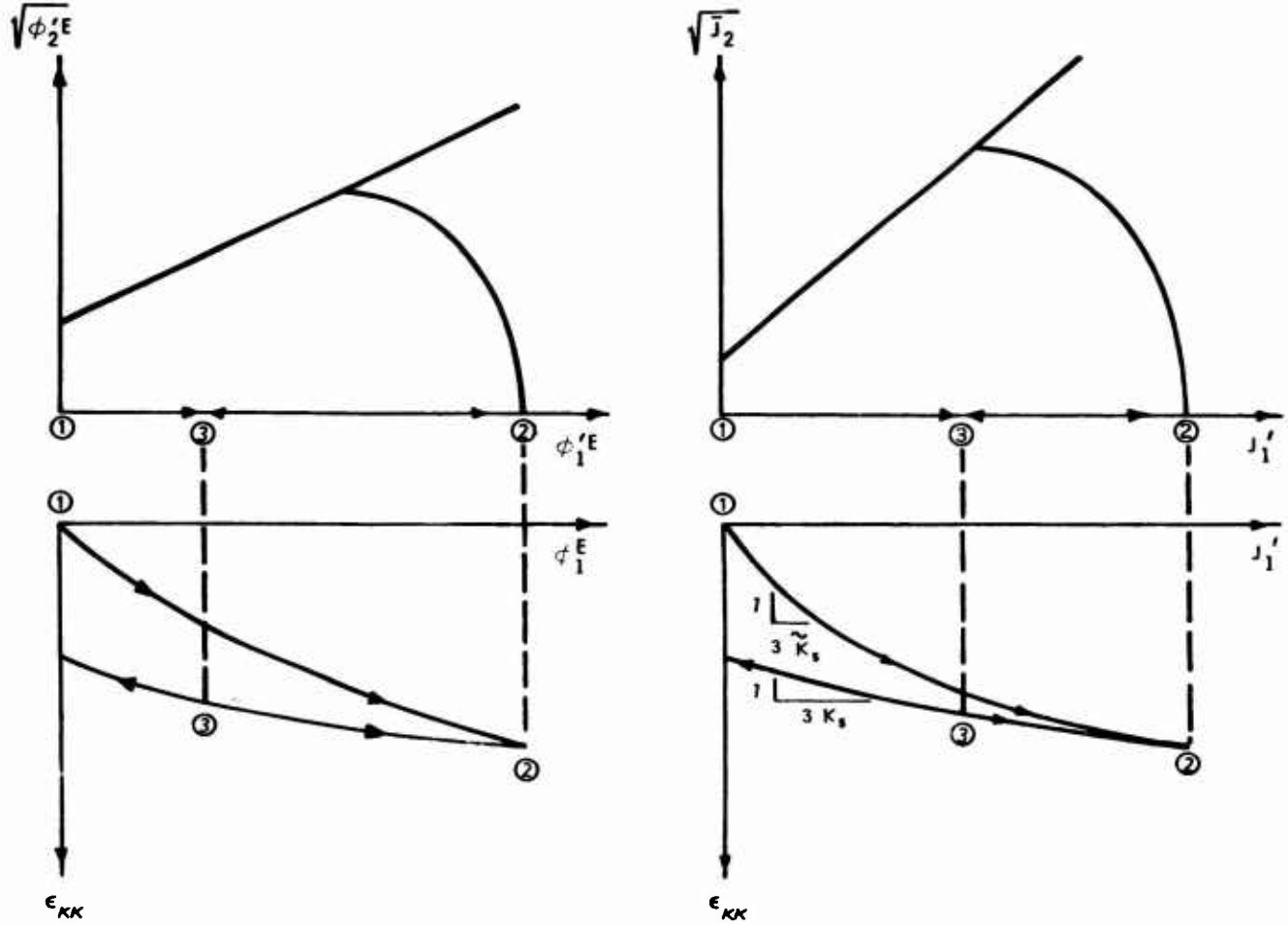

Figure 15. Behavior of the model under drained hydrostatic compression (isotropic consolidation)

$$\frac{dJ_1'}{d\varepsilon_{kk}} = \frac{1}{\frac{1}{3\left(\frac{3}{1+2\alpha_s^E}\right)^2 B_s} + D_s\left(\frac{1+2\alpha_s^P}{3}\right)\left(W_s - \varepsilon_{kk}^P\right)} = 3\tilde{K}_s \qquad (54)$$

where $\tilde{K}_s$ is the apparent bulk modulus of the anisotropic material under drained hydrostatic loading. The second term in the denominator of Equations 52 and 54 produces a softening of the apparent bulk modulus due to plastic volumetric compaction. At high pressures, the softening term goes to zero (i.e., $\varepsilon_{kk}^P \simeq W_s$) and the apparent modulus $\tilde{K}_s$ approaches the elastic bulk modulus, $K_s = \left[9/(1+2\alpha_s)^2\right]B_s$. Also, if a sample is first isotropically consolidated (from point 1 to point 2 in Figure 15), then unloaded (point 2 to point 3), and then reloaded (point 3 to point 2), the model dictates that the unloading-reloading behavior is purely elastic.

Undrained condition

25. During an undrained hydrostatic loading, the effective stresses generally are not zero. The total stress-strain relations for this drainage condition can be obtained in a manner similar to that used to derive Equations 40 through 50, except that they will involve the total stresses (Equations 25, 27, 28, 30, 32 and 34) instead of the effective stresses, and the model coefficients will have the subscript m (mixture) instead of the subscript s (skeleton) (Table 2); thus:

$$\varepsilon_{kk}^E = \left(\frac{1+2\alpha_m^E}{9}\right)\left(\frac{1-B_{1m}}{B_{2m}\,B_{im}}\right)\ln\left[\frac{\exp\left(B_{2m}\,\phi_1^E\right) - B_{1m}}{1-B_{1m}}\right] \qquad (55)$$

$$\varepsilon_r^E = \frac{\alpha_m^E}{9}\left(\frac{1-B_{1m}}{B_{2m}\,B_{im}}\right)\ln\left[\frac{\exp\left(B_{2m}\,\phi_1^E\right) - B_{1m}}{1-B_{1m}}\right] \qquad (56)$$

$$\varepsilon_z^E = \frac{1}{9}\left(\frac{1 - B_{1m}}{B_{2m}\, B_{im}}\right) \ln\left[\frac{\exp\left(B_{2m}\, \phi_1^E\right) - B_{1m}}{1 - B_{1m}}\right] \tag{57}$$

$$\varepsilon_{kk}^P = W_m \left\{1 - \exp\left[-\left(1 + 2\alpha_m^P\right) D_m\, \phi_1^E \Big/ \left(1 + 2\alpha_m^E\right)\right]\right\} \tag{58}$$

$$\varepsilon_r^P = \left(\frac{\alpha_m^P}{1 + 2\alpha_m^P}\right) W_m \left\{1 - \exp\left[-\left(1 + 2\alpha_m^P\right) D_m\, \phi_1^E \Big/ \left(1 + 2\alpha_m^E\right)\right]\right\} \tag{59}$$

$$\varepsilon_z^P = \left(\frac{W_m}{1 + 2\alpha_m^P}\right) \left\{1 - \exp\left[-\left(1 + 2\alpha_m^P\right) D_m\, \phi_1^E \Big/ \left(1 + 2\alpha_m^E\right)\right]\right\} \tag{60}$$

$$\varepsilon_r = \frac{\alpha_m^E}{9}\left(\frac{1 - B_{1m}}{B_{2m}\, B_{im}}\right) \ln\left[\frac{\exp\left(B_{2m}\, \phi_1^E\right) - B_{1m}}{1 - B_{1m}}\right] + \left(\frac{W_m\, \alpha_m^P}{1 + 2\alpha_m^P}\right) \left\{1 - \exp\left[-\left(1 + 2\alpha_m^P\right) D_m\, \phi_1^E \Big/ \left(1 + 2\alpha_m^E\right)\right]\right\} \tag{61}$$

$$\varepsilon_z = \frac{1}{9}\left(\frac{1 - B_{1m}}{B_{2m}\, B_{im}}\right) \ln\left[\frac{\exp\left(B_{2m}\, \phi_1^E\right) - B_{1m}}{1 - B_{1m}}\right] + \left(\frac{W_m}{1 + 2\alpha_m^P}\right) \left\{1 - \exp\left[-\left(1 + 2\alpha_m^P\right) D_m\, \phi_1^E \Big/ \left(1 + 2\alpha_m^E\right)\right]\right\} \tag{62}$$

and

$$\varepsilon_{kk} = \left(\frac{1 + 2\alpha_m^E}{9}\right)\left(\frac{1 - B_{1m}}{B_{2m}\, B_{im}}\right) \ln\left[\frac{\exp\left(B_{2m}\, \phi_1^E\right) - B_{1m}}{1 - B_{1m}}\right] + W_m \left\{1 - \exp\left[-\left(1 + 2\alpha_m^P\right) D_m\, \phi_1^E \Big/ \left(1 + 2\alpha_m^E\right)\right]\right\} \tag{63}$$

Computation of effective
stress and pore pressure

26. The effective stresses and the pore pressures generated during undrained hydrostatic loading can be computed by the assumption that the volumetric strains from Equations 50 and 63 are equal (procedure a of paragraph 21), thus:

$$\left(\frac{1 + 2\alpha_s^E}{9}\right)\left(\frac{1 - B_{1s}}{B_{2s}\ B_{is}}\right) \ln\left[\frac{\exp\left(B_{2s}\ \phi_1'^E\right) - B_{1s}}{1 - B_{1s}}\right] + W_s\left\{1 - \exp\left[-\left(1 + 2\alpha_s^P\right) D_s\ \phi_1'^E \Big/ \left(1 + 2\alpha_s^E\right)\right]\right\}$$

$$= \left(\frac{1 + 2\alpha_m^E}{9}\right)\left(\frac{1 - B_{1m}}{B_{2m}\ B_{im}}\right) \ln\left[\frac{\exp\left(B_{2m}\ \phi_1^E\right) - B_{1m}}{1 - B_{1m}}\right] + W_s\left\{1 - \exp\left[-\left(1 + 2\alpha_m^P\right) D_m\ \phi_1^E \Big/ \left(1 + 2\alpha_m^E\right)\right]\right\} \quad (64)$$

from which $\phi_1'^E$ can be obtained as a function of ϕ_1^E. The effective stresses and the pore pressure, u, become (see Equations 4 and 29)

$$\sigma_z' = \sigma_r' = \frac{\phi_1'^E}{1 + 2\alpha_s^E} \quad (65)$$

$$u = \sigma_z - \sigma_z' = \sigma_r - \sigma_r' \quad (66)$$

Note that when the material is fully saturated (i.e., a two-phase system) and the water is assumed to be incompressible, the right sides of Equations 63 and 64 become zero, i.e., $\phi_1'^E$ is independent of ϕ_1^E and Equation 64 can be satisfied if and only if $\phi_1'^E$ is equal to zero. This means that all of the applied load is carried by the water.

Shear Phase

27. During the shear phase of a conventional triaxial test, the cell pressure is maintained constant:

$$\sigma_r = \text{constant} = P_c \tag{67}$$

$$d\sigma_r = 0 \tag{68}$$

where P_c is the confining pressure at the end of the hydrostatic compression phase. If it is assumed that the hydrostatic compression phase that preceded the shear phase was drained, the confining pressure, P_c, is effective and is equal to P'_c, the effective confining pressure.

Drained condition

28. During the subsequent drained shear phase, effective and total stresses are equal (i.e., the effective stress path is known and is identical to the total stress path). The material response is determined from Equation C40 of Appendix C by use of the response functions and the material parameters listed in Table 2 for the drained condition; thus,

$$d\varepsilon_{ij} = \frac{1}{9B_s} d\phi_1'^{E} A_{ij}'^{E} + \frac{1}{2S_s} d\eta_{ij}'^{E} + \frac{\Lambda_s}{\zeta_s} \left[\frac{\partial \delta_s}{\partial \phi_1'^{P}} A_{ij}'^{P} + \frac{\eta_{ij}'^{P}}{2\sqrt{\phi_2'^{P}}} \frac{\partial \delta_s}{\partial \sqrt{\phi_2'^{P}}} \right] \tag{69}$$

where

$$A_{ij}'^{E} = \begin{bmatrix} 1 & 0 & 0 \\ 0 & \alpha_s^E & 0 \\ 0 & 0 & \alpha_s^E \end{bmatrix} \tag{70}$$

$$\eta_{ij}'^{E} = \frac{\partial \phi_2'^{E}}{\partial \sigma_{ij}'} \quad \text{(see Equations B14 and B15 of Appendix B)} \tag{71}$$

$$\delta_s = \begin{cases} F\left(\phi_1'^P \, , \sqrt{\phi_2'^P} \, , \kappa_s\right) & \text{on the hardening surface} \\ f\left(\phi_1'^P \, , \sqrt{\phi_2'^P}\right) & \text{on the failure surface} \end{cases} \tag{72}$$

$$A_{ij}'^P = \begin{bmatrix} 1 & 0 & 0 \\ 0 & \alpha_s^P & 0 \\ 0 & 0 & \alpha_s^P \end{bmatrix} \tag{73}$$

and

$$\eta_{ij}'^P = \frac{\partial \phi_2'^P}{\partial \sigma_{ij}'} \tag{74}$$

Equations C38 and C39 of Appendix C can be used to calculate Λ_s and ζ_s, respectively, using the material parameters for the drained condition (Table 2).

29. The volumetric strain can be obtained from Equation 69 by multiplication of both sides by the Kronecker delta, δ_{ij}:

$$d\varepsilon_{kk} = \frac{1 + 2\alpha_s^E}{9B_s} d\phi_1'^E + \frac{\Lambda_s}{\zeta_s}\left(1 + 2\alpha_s^P\right)\frac{\partial \delta_s}{\partial \phi_1'^P} \tag{75}$$

Typical (qualitative) results predicted by the model for a drained shear test are shown in Figure 16.

Undrained condition

30. During an undrained shear test (following isotropic consolidation) only the total stress path and, consequently, the total stresses are known. The material response for this phase can be determined in a manner similar to that used to develop Equations 69 through 75, except that they involve the total stresses (Equations 25, 27, 28, 30, 32 and 34) instead of the effective stresses, and the model coefficients will have the subscript m (mixture) instead of the subscript s (skeleton); thus,

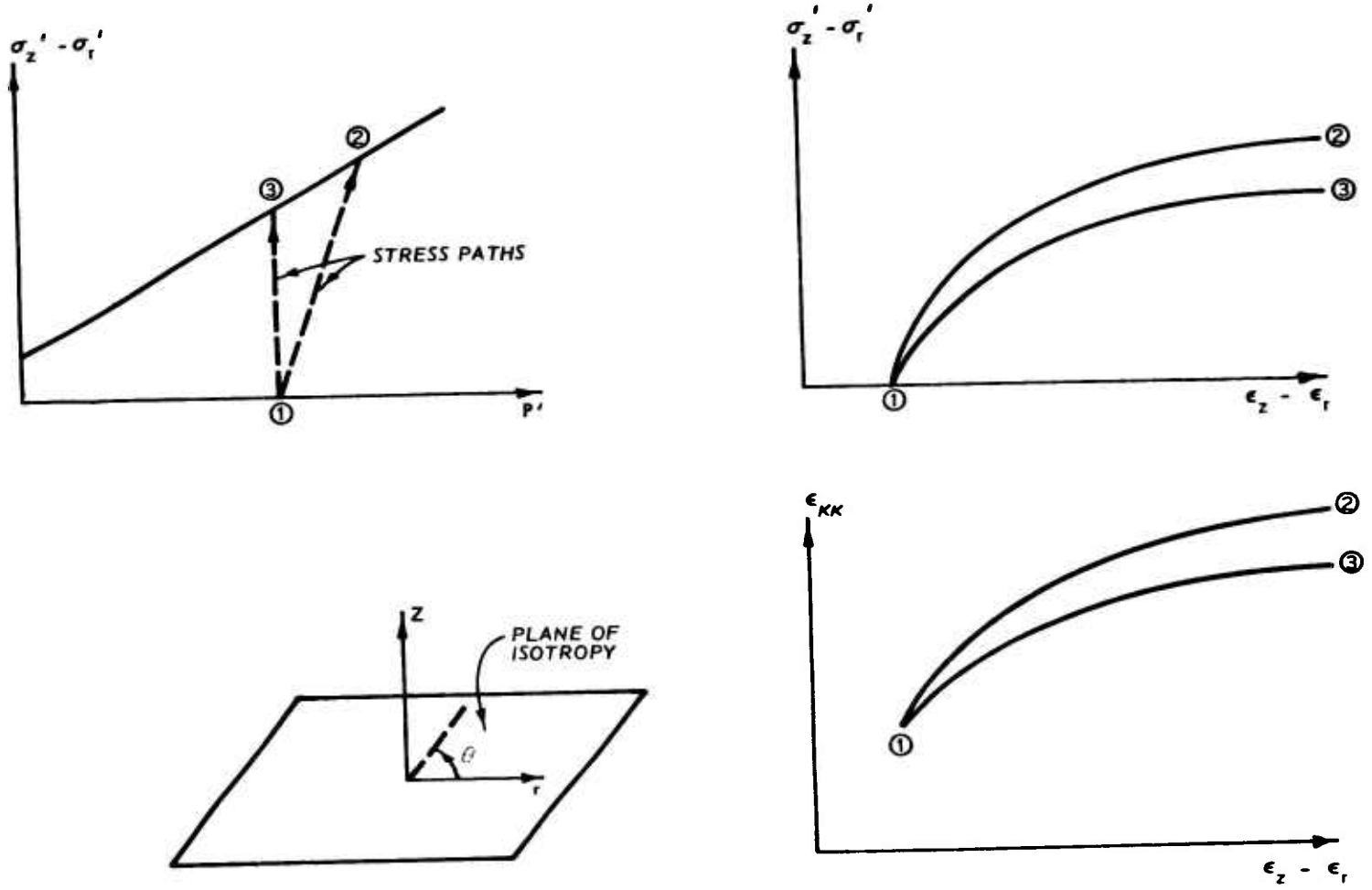

Figure 16. Drained shear behavior predicted by the model for a conventional triaxial test and a constant mean normal stress test

$$d\varepsilon_{ij} = \frac{1}{9B_m} d\phi_1^E A_{ij}^E + \frac{1}{2S_m} d\eta_{ij}^E + \frac{\Lambda_m}{\zeta_m} \left[\frac{\partial \mathcal{f}_m}{\partial \phi_1^P} A_{ij}^P + \frac{\eta_{ij}^P}{2\sqrt{\phi_2^P}} \frac{\partial \mathcal{f}_m}{\partial \sqrt{\phi_2^P}} \right] \tag{76}$$

and the volumetric strain increment is

$$d\varepsilon_{kk} = \frac{1 + 2\alpha_m^E}{9B_m} d\phi_1^E + \frac{\Lambda_m}{\zeta_m} \left(1 + 2\alpha_m^P\right) \frac{\partial \mathcal{f}_m}{\partial \phi_1^P} \tag{77}$$

where

$$A_{ij}^E = \begin{bmatrix} 1 & 0 & 0 \\ 0 & \alpha_m^E & 0 \\ 0 & 0 & \alpha_m^E \end{bmatrix} \tag{78}$$

$$\eta_{ij}^E = \frac{\partial \phi_2^E}{\partial \sigma_{ij}} \quad \text{(see Equations B14 and B15 of Appendix B)} \tag{79}$$

$$\mathcal{f}_m = \begin{cases} F\left(\phi_1^P, \sqrt{\phi_2^P}, \kappa_m\right) & \text{on the hardening surface} \\ f\left(\phi_1^P, \sqrt{\phi_2^P}\right) & \text{on the failure surface} \end{cases} \tag{80}$$

$$A_{ij}^P = \begin{bmatrix} 1 & 0 & 0 \\ 0 & \alpha_m^P & 0 \\ 0 & 0 & \alpha_m^P \end{bmatrix} \tag{81}$$

and

$$\eta_{ij}^P = \frac{\partial \phi_2^P}{\partial \sigma_{ij}} \tag{82}$$

Equations C38 and C39 of Appendix C can be used to calculate Λ_m and ζ_m, respectively, using the material parameters for the undrained condition (Table 2).

Effective stress and
pore pressure computations

31. During the undrained shear test, the effective stresses and the pore pressure at the end of each loading increment can be computed by the assumption that the total volumetric strain increments obtained from Equations 75 and 77 are equal (i.e., procedure a of paragraph 21); thus,

$$\frac{1 + 2\alpha_s^E}{9B} d\phi_1'^E + \frac{\Lambda_s}{\zeta_s}\left(1 + 2\alpha_s^P\right)\frac{\partial \zeta_s}{\partial \phi_1'^P} = \frac{1 + 2\alpha_m^E}{9B_m} d\phi_1^E + \frac{\Lambda_m}{\zeta_m}\left(1 + 2\alpha_m^P\right)\frac{\partial \zeta_m}{\partial \phi_1^P} \quad (83)$$

from which $\phi_1'^E$ can be obtained as a function of ϕ_1^E. The pore pressure and the effective stresses then become (see Equations 4 and 29):

$$u = \frac{\sigma_z + 2\alpha_s^E \sigma_r - \phi_1'^E}{1 + 2\alpha_s^E} = \frac{\sigma_z + 2\alpha_s^P \sigma_r - \phi_1'^P}{1 + 2\alpha_s^P} \quad (84)$$

$$\sigma_z' = \sigma_z - u \quad (85)$$

$$\sigma_r' = \sigma_r - u \quad (86)$$

Since the effective stresses are known, the total strain increment tensor for the undrained condition can be computed from Equation 69. Typical (qualitative) results predicted by the model for undrained shear are shown in Figure 17. Figure 17 also depicts qualitatively the effects of the parameter R on the stress-strain-pore pressure response during a conventional undrained triaxial shear test.

32. When the material is fully saturated (i.e., two-phase system) and the water is assumed to be incompressible, the right sides of Equations 77 and 83 become zero; i.e., $\phi_1'^E$ is independent of ϕ_1^E. This means that the effective stress path is independent of the total stress path applied to the material. This behavior is also predicted by the isotropic model reported in Reference 10.

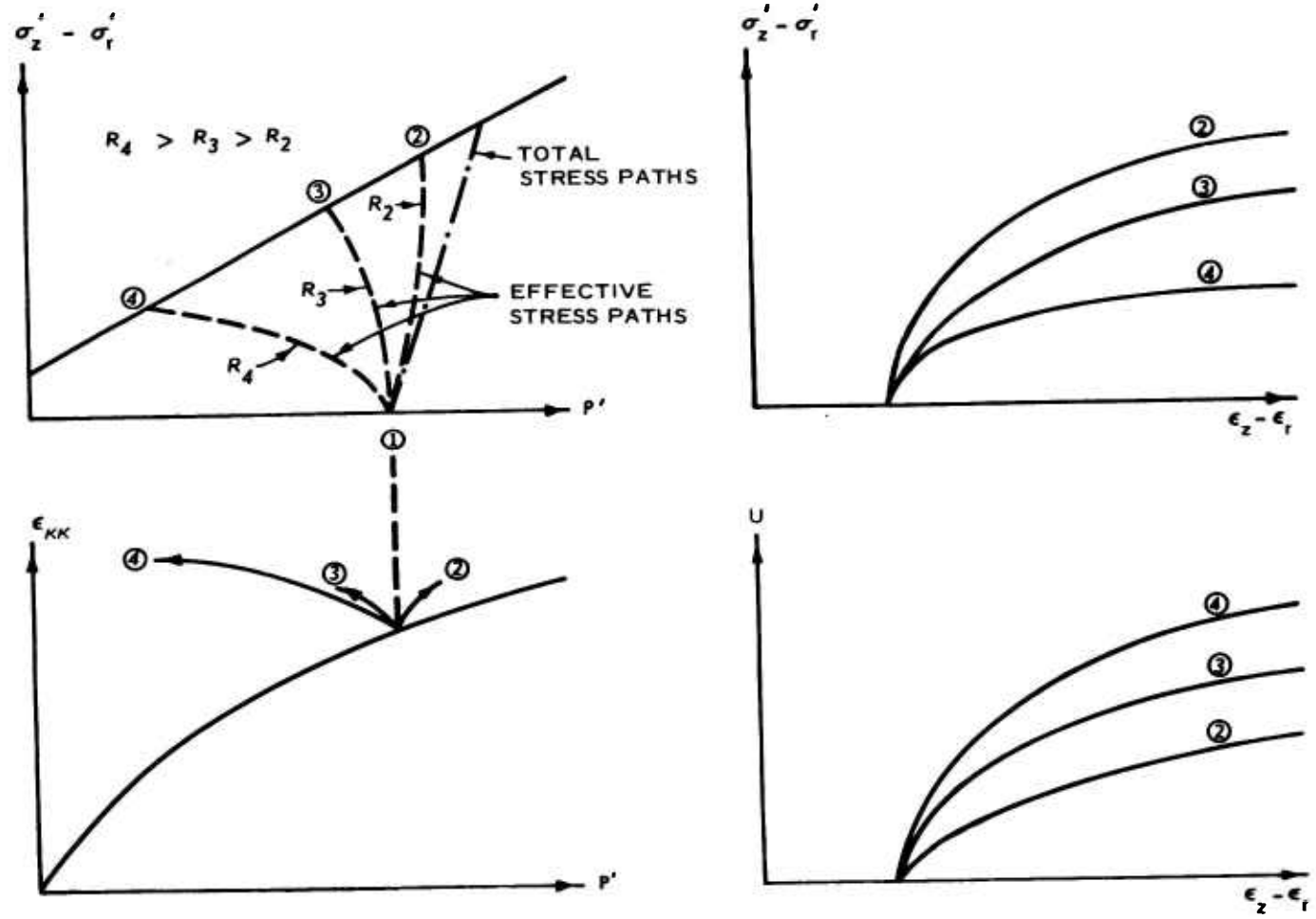

Figure 17. Undrained shear behavior predicted by the model, showing the influence of the parameter R on the effective stress path in a conventional undrained triaxial test

PART VI: SUMMARY AND RECOMMENDATIONS

Summary

33. A three-dimensional, elastic-plastic work-hardening constitutive relationship for transverse-isotropic three-phase earth materials has been developed. Within the elastic range, the constitutive relationship contains three dimensionless parameters and two response functions. In the plastic range, it contains three dimensionless parameters and three potential functions. The numerical values of the elastic and plastic parameters, as well as the values of the coefficients in the response and potential functions, can be determined experimentally using essentially conventional soil testing techniques.

34. The constitutive relationship is capable of simulating the drained and undrained behavior of typical earth materials subjected to both spherical and deviatoric states of stress. Moreover, it reduces to its isotropic counterpart without any change in the forms of its mathematical functions.

35. The behavior of the model under drained and undrained triaxial test conditions has been examined and a method for obtaining the effective and total stresses, as well as the pore pressure of a multiphase soil for given total stress or strain paths, has been outlined.

Recommendations

36. It is recommended that this constitutive model be incorporated into a numerical computer program that simulates cylindrical and cubical triaxial test boundary conditions so that the behavior of the model can be correlated with experimental data for three-phase isotropic and/or transverse-isotropic earth media. Such a computer program is necessary for studying the effects of the individual model parameters on the behavior of the model.

37. It is further recommended that the constitutive relationship be incorporated into a suitable numerical computer code for use in performing effective stress analyses of earth structures boundary-value problems.

REFERENCES

1. Taylor, D. W., Fundamentals of Soil Mechanics, pp 12-21, 1948, Wiley, New York.

2. Baladi, G. Y. and Hadala, P. F., "Ground Shock Calculation Parameter Study; Effect of Various Nonlinear Elastic-Plastic Model Formulations," Technical Report S-71-4, Report 1, Apr 1971, U. S. Army Engineer Waterways Experiment Station, CE, Vicksburg, Miss.

3. Baladi, G. Y. and Nelson, I., "Ground Shock Calculation Parameter Study; Influence of Type of Constitutive Model on Ground Motion Calculations," Technical Report S-71-4, Report 3, Apr 1974, U. S. Army Engineer Waterways Experiment Station, CE, Vicksburg, Miss.

4. Nelson, I., "Investigation of Ground Shock Effects in Nonlinear Hysteretic Media; Modeling the Behavior of a Real Soil," Contract Report S-68-1, Report 2, Jul 1970, U. S. Army Engineer Waterways Experiment Station, CE, Vicksburg, Miss.; prepared by Paul Weidlinger under Contract No. DACA 39-67-C-0098.

5. Nelson, I. and Baladi, G. Y., "Outrunning Ground Shock Computed with Different Models," Journal, Engineering Mechanics Division, American Society of Civil Engineers, Vol 103, No. EM3, Jun 1977, pp 377-393.

6. Baladi, G. Y., "The Latest Development in the Nonlinear Elastic-Nonideally Plastic Work Hardening Cap Model," Symposium on Plasticity and Soil Mechanics, Cambridge, England, 1973, pp 51-55.

7. Sandler, I. S., DiMaggio, F. L., and Baladi, G. Y., "Generalized Cap Model for Geological Materials," Journal, Geotechnical Engineering Division, American Society of Civil Engineers, Vol 102, No. GT7, Jul 1976, pp 683-699.

8. Baladi, G. Y., "Numerical Implementation of a Transverse-Isotropic Inelastic, Work-Hardening Constitutive Model," Transactions, 4th International Conference on Structural Mechanics in Reactor Technology, Methods for Structural Analysis, Vol M, 1977.

9. Schofield, A. and Wroth, P., Critical State Soil Mechanics, McGraw-Hill, New York, 1968.

10. Baladi, G. Y. and Rohani, B., "Liquefaction Potential of Dams and Foundations; Development of an Elastic-Plastic Constitutive Relationship for Saturated Sand," Research Report S-76-2, Report 3, Feb 1977, U. S. Army Engineer Waterways Experiment Station, CE, Vicksburg, Miss.

11. Terzaghi, K. and Peck, R. B., Soil Mechanics in Engineering Practice, Wiley, New York, 1948.

12. Bishop, A. W. et al., "Factors Controlling the Strength of Partly Saturated Cohesive Soils," Research Conference on Shear Strength of Cohesive Soils, American Society of Civil Engineers, 1960, pp 503-532.

13. Croney, D., Coleman, J. D., and Black, W. P. M., "Movement and Distribution of Water in Soil in Relation to Highway Design and Performance," Highway Research Board Special Report 40, pp 226-252, 1958.

14. Aitchison, G. D., "Relationships of Moisture Stress and Effective Stress Functions in Unsaturated Soils," Pore Pressure and Suction in Soils, Butterworths, London, 1961, pp 47-53.

15. Hill, R., The Mathematical Theory of Plasticity, Clarendon Press, Oxford, England, 1950.

16. Love, A. E. H., Mathematical Theory of Elasticity, 4th ed., Cambridge University Press, Cambridge, England, 1934.

17. Lekhnitskii, S. G., Theory of Elasticity of an Anisotropic Elastic Body, Holden-Day, San Francisco, 1963.

18. Guillemin, E. A., The Mathematics of Circuit Analysis, Wiley, New York, 1949.

19. Drucker, D. C., "On Uniqueness in the Theory of Plasticity," Quarterly of Applied Mathematics, Vol 14, 1956.

20. Prager, W., Introduction to Mechanics of Continua, Ginn, Boston, 1961.

21. Handelman, G. H. et al., "On the Mechanical Behavior of Metals in the Strain-Hardening Range," Quarterly of Applied Mathematics, Vol 4, 1947, pp 397-407.

Table 1

Summary of Model Parameters for a Single-Phase System

Parameters	Response Functions	Equation Number	Material Constants
Elastic pseudo stress invariants*	ϕ_1^E ϕ_2^E	B13	α^E β^E , γ^E
Elastic response functions*	$B\left(\phi_1^E , \varepsilon_{kk}^P\right)$ $S\left(\sqrt{\phi_2^E} , \varepsilon_{kk}^P\right)$	8 or 9 10	B_i , B_1 , B_2 S_i , S_1 , S_2 S_3 , S_4
Plastic pseudo stress invariants	ϕ_1^P ϕ_2^P	C14	α^P β^P , γ^P
Plastic potential functions	$f\left(\phi_1^P , \sqrt{\phi_2^P}\right)$ $F\left(\phi_1^P , \sqrt{\phi_2^P} , \kappa\right)$	12 13	ψ , k R_i , R_1 , R_2
Plastic hardening function	$X(\kappa) = X\left(\varepsilon_{kk}^P\right)$	16	W , D

* Note that when $\alpha^E = \beta^E = \gamma^E = \alpha^P = \beta^P = \gamma^P = 1$, ϕ_1^E and ϕ_1^P are equal and become J_1 , the familiar first invariant of the stress tensor, and ϕ_2^E and ϕ_2^P are equal and become $\bar{J}_2$, the familiar second invariant of the stress deviation tensor. In addition, B becomes K, and S becomes G , the bulk and shear moduli of the material, respectively.

Table 2

Summary of Model Parameters for a Multiphase System

	Set 1 Soil Skeleton (Drained Condition)		Set 2 Solid Particles, Water and Gas Mixture (Undrained Condition)	
	Response Functions	Material Constants	Response Functions	Material Constants
Elastic pseudo stress invariants	$\phi_1'^E$ $\phi_2'^E$	α_s^E , β_s^E , γ_s^E	ϕ_1^E ϕ_2^E	α_m^E , β_m^E , γ_m^E
Elastic response functions*	$B_s\left(\phi_1'^E , \epsilon_{kk}^P\right)$ $S_s\left(\sqrt{\phi_2'^E} , \epsilon_{kk}^P\right)$	B_{is} , B_{1s} , B_{2s} S_{is} , S_{1s} , S_{2s} , S_{3s} , S_{4s}	$B_m\left(\phi_1^E , \epsilon_{kk}^P\right)$ $S_m\left(\sqrt{\phi_2^E} , \epsilon_{kk}^P\right)$	B_{im} , B_{1m} , B_{2m} S_{im} , S_{1m} , S_{2m} , S_{3m} , S_{4m}
Plastic pseudo stress invariants	$\phi_1'^P$ $\phi_2'^P$	α_s^P , β_s^P , γ_s^P	ϕ_1^P ϕ_2^P	α_m^P , β_m^P , γ_m^P
Plastic potential functions*	$g\left(\phi_1'^P , \sqrt{\phi_2'^P}\right)$ $F\left(\phi_1'^P , \sqrt{\phi_2'^P} , \kappa_s\right)$	ψ_s , k_s R_{is} , R_{1s} , R_{2s}	$g\left(\phi_1^P , \sqrt{\phi_2^P}\right)$ $F\left(\phi_1^P , \sqrt{\phi_2^P} , \kappa_m\right)$	ψ_m , k_m R_{im} , R_{1m} , R_{2m}
Plastic hardening function	$X(\kappa_s)$	W_s , D_s	$X(\kappa_m)$	W_m , D_m

* The mathematical forms of these response functions are identical to those shown in Table 1.

APPENDIX A: BASIC CONCEPTS FROM CONTINUUM MECHANICS

1. From a microscopic point of view, physical bodies are composed of discrete molecules interconnected by some internal forces of mutual attraction and repulsion. The concept of stress within a body requires that boundary distances and/or loaded areas be large in comparison with distances between molecules and/or the size of the individual molecule. This, in effect, transforms a body composed of discrete molecules into a statistically macroscopic equivalent amenable to mathematical analysis. Since most engineering problems deal with macroscopic phenomena and involve boundary distances and loaded areas very large compared with individual molecules, it appears reasonable and convenient to invoke the mechanics of continua as the basis for analytical consideration of these problems.

2. The theory of continuous media is built upon two strong foundations: basic balance and conservation laws and constitutive theory. The basic balance and conservation laws of any continuum are

a. Conservation of mass
b. Conservation of energy
c. Balance of linear momentum
d. Balance of angular momentum
e. Inadmissibility of decreasing entropy

When thermal effects are neglected, the above basic axioms of continuum mechanics lead to the following continuity equation:*

$$\frac{\partial \rho}{\partial t} + (\rho v_i)_{,i} = 0 \tag{A1}$$

and the equations of motion:

$$\sigma_{ij,j} + F_i - \rho a_i = 0 \tag{A2}$$

---

* Indices take on values 1, 2, or 3. A repeated index is to be summed over its range. A comma between subscripts represents a derivative. Quantities are referred to rectangular Cartesian coordinates X_i .

where

ρ = mass density

t = time

v_i = components of velocity vector

$\sigma_{ij} = \sigma_{ji}$ = symmetrical stress tensor

F_i = components of body force

a_i = components of acceleration vector

3. Equations A1 and A2 are called field equations. They constitute four equations that involve ten unknown functions of time and space. Therefore, the system resulting from Equations A1 and A2 is indeterminate. These unknown functions are: the mass density, ρ, the three velocity components, v_i, and the six independent stress components, σ_{ij}. The body force components, F_i, are known quantities and the acceleration components, a_i, are expressible in terms of the velocity components, v_i. To overcome the indeterminacy and make the system complete, six additional expressions relating the ten unknown variables are required. In continuum mechanics, such relations are stated by constitutive equations (or material models), which relate stresses to deformation and history of deformation. The difference between constitutive equations and field equations (Equations A1 and A2) is that the latter contain both space coordinates and time, and are applicable to all materials, whereas the former are independent of space coordinates (for homogeneous materials) and represent the intrinsic response of a particular material or class of materials and, as such, are mathematical idealizations of the mechanical behavior of real materials.

4. The general form of a constitutive equation may be expressed by the following functional form:

$$H_{ij}\left(D_{mn}, r_{qp}, \epsilon_{rs}, \sigma_{\ell k}, \rho\right) = 0 \qquad \text{(A3)}$$

where the deformation-rate tensor, D_{mn}, and the spin tensor, r_{qp}, are related to the components of the velocity vector, v_i, by

$$D_{mn} = \frac{1}{2}\left(v_{m,n} + v_{n,m}\right)$$

and (A4)

$$r_{qp} = \frac{1}{2}\left(v_{q,p} - v_{p,q}\right)$$

and the infinitesimal strain tensor, ε_{rs}, is related to the components of displacement vector, u_i, by

$$\varepsilon_{rs} = \frac{1}{2}\left(u_{r,s} + u_{s,r}\right) \tag{A5}$$

Equations A1 through A3 constitute ten equations involving ten unknown variables. These equations will lead, in conjunction with the kinematic relations given by Equations A4 and A5, and the appropriate boundary conditions, to a complete description for the solution of a boundary-value problem.

5. In general, materials having the same mass and geometry respond differently when subjected to identical external effects. Therefore, a variety of constitutive theories has emerged, each of which describes a limited number of physical phenomena decided on at the outset for a given material. In Appendix B of this report, the constitutive theory for a linear elastic transverse-isotropic material is documented. In Appendix C the constitutive theory for an elastic-plastic transverse-isotropic material is presented.

APPENDIX B: LINEAR ELASTIC TRANSVERSE-ISOTROPIC CONSTITUTIVE MODEL

1. Linear elastic constitutive models have been widely used to approximate the mechanical behavior of a large number of engineering materials. This type of constitutive model implies that the state of stress is proportional to the current state of strain. The most general form of such a linear relationship is

$$\epsilon_{ij} = \overline{C}_{ijk\ell}\, \sigma_{k\ell} \tag{B1}$$

where $\overline{C}_{ijk\ell}$ = the elastic compliances (moduli) of the material, which are 81 in number . The coefficients $\overline{C}_{ijk\ell}$ in Equation B1 generally vary from point to point within the medium. If, however, the $\overline{C}_{ijk\ell}$ are independent of the position of the point, the medium is termed "homogeneous." Equation B1 is a natural generalization of Hooke's law, and it is used in all developments of the linear theory of elasticity.

2. Since the stress and strain tensors are symmetric, the indices i and j in Equation B1 can be interchanged, which reduces[16*] the number of independent compliances from 81 to 54; i.e., the relation

$$\overline{C}_{ijk\ell} = \overline{C}_{jik\ell} \tag{B2}$$

represents 27 equalities. Furthermore, the indices k and ℓ can be interchanged, which reduces the number of independent relations by 18, as expressed by the equalities

$$\overline{C}_{ijk\ell} = \overline{C}_{ij\ell k} \tag{B3}$$

Hence, the maximum number of independent constants contained in Equation B1 is at most 36.

---

* Raised numbers refer to items listed in the References at the end of the main text.

3. The number of independent elastic constants in Equation B1 can be further reduced from 36 to 21 whenever there exists a function[16]

$$\overline{W} = \frac{1}{2} \sigma_{ij} \varepsilon_{ij} \tag{B4}$$

with the property that

$$\varepsilon_{ij} = \frac{\partial \overline{W}}{\partial \sigma_{ij}} \tag{B5}$$

The potential function, $\overline{W}$, is called the "complementary energy function." Its existence for isothermal and adiabatic processes has been argued on the basis of the first and second laws of thermodynamics. For the most general case of a linear anisotropic elastic body, the number of independent elastic constants (Equation B1) is 21. If the medium is elastically symmetric in certain directions, the number of independent constants, $\overline{C}_{ijk\ell}$, can be even further reduced.

4. For a linear elastic transversely-isotropic material that has equivalent properties in all directions in the 22-33 plane of a 11-22-33 coordinate system, i.e., where the 11-axis is an axis of symmetry of an infinitely large order (Figure 5), it can be shown[17] that only five independent compliances exist. For such a material, Equation B1 becomes

$$\begin{bmatrix} \varepsilon_{11} \\ \varepsilon_{22} \\ \varepsilon_{33} \\ \varepsilon_{12} \\ \varepsilon_{13} \\ \varepsilon_{23} \end{bmatrix} = \begin{bmatrix} C_{11} & C_{12} & C_{12} & 0 & 0 & 0 \\ C_{12} & C_{22} & C_{23} & 0 & 0 & 0 \\ C_{12} & C_{23} & C_{22} & 0 & 0 & 0 \\ 0 & 0 & 0 & C_{44} & 0 & 0 \\ 0 & 0 & 0 & 0 & C_{44} & 0 \\ 0 & 0 & 0 & 0 & 0 & C_{22} - C_{23} \end{bmatrix} \begin{bmatrix} \sigma_{11} \\ \sigma_{22} \\ \sigma_{33} \\ \sigma_{12} \\ \sigma_{13} \\ \sigma_{23} \end{bmatrix} \tag{B6}$$

where $C_{11} = \overline{C}_{1111}$, $C_{12} = \overline{C}_{1122} = \overline{C}_{1133}$, $C_{22} = \overline{C}_{2222} = \overline{C}_{3333}$, $C_{23} = \overline{C}_{2233}$, and $C_{44} = \overline{C}_{1212} = \overline{C}_{1313}$. The remaining $\overline{C}_{ijk\ell}$ coefficients are zero.

5. To ensure uniqueness of solution for a boundary-value problem involving the material described by Equation B6, the complementary energy function (Equation B4) must be positive and definite. This is ensured[18] if, and only if, the determinant of the coefficients of Equation B6 and all of its principal minors are positive, i.e., the following conditions must hold:[17]

$$\left.\begin{aligned} C_{11} &> 0 \\ C_{22} &> 0 \\ C_{44} &> 0 \\ C_{22} - C_{23} &> 0 \\ C_{22}^2 - C_{23}^2 &> 0 \\ (C_{22} + C_{23})\, C_{11} - 2C_{12}^2 &> 0 \end{aligned}\right\} \tag{B7}$$

6. Equation B6 may also be written in the following familiar form:[17]

$$\begin{bmatrix} \varepsilon_{11} \\ \varepsilon_{22} \\ \varepsilon_{33} \\ \varepsilon_{12} \\ \varepsilon_{13} \\ \varepsilon_{23} \end{bmatrix} = \begin{bmatrix} \frac{1}{E'} & -\frac{\nu'}{E'} & -\frac{\nu'}{E'} & 0 & 0 & 0 \\ -\frac{\nu'}{E'} & \frac{1}{E} & -\frac{\nu}{E} & 0 & 0 & 0 \\ -\frac{\nu'}{E'} & -\frac{\nu}{E} & \frac{1}{E} & 0 & 0 & 0 \\ 0 & 0 & 0 & \frac{1}{2G'} & 0 & 0 \\ 0 & 0 & 0 & 0 & \frac{1}{2G'} & 0 \\ 0 & 0 & 0 & 0 & 0 & \frac{1}{2G} \end{bmatrix} \begin{bmatrix} \sigma_{11} \\ \sigma_{22} \\ \sigma_{33} \\ \sigma_{12} \\ \sigma_{13} \\ \sigma_{23} \end{bmatrix} \tag{B8}$$

Conditions B7 become

$$\left.\begin{aligned} E &> 0 \\ E' &> 0 \\ G' &> 0 \\ G &> 0 \\ -1 < \nu &< 1 \\ \frac{E'(1-\nu)}{E} - 2(\nu')^2 &> 0 \end{aligned}\right\} \qquad \text{(B9)}$$

where

ν = Poisson's ratio that characterizes the transverse reduction in the plane of isotropy (the 22-33 plane, Figure 5) due to stress in the same plane

ν' = Poisson's ratio that characterizes the transverse reduction in the plane of isotropy due to stress normal to it

E = Young's modulus in the plane of isotropy

E' = Young's modulus in a plane normal to the plane of isotropy

$G = E/2(1 + \nu)$ = shear modulus for the plane of isotropy

G' = shear modulus for a plane normal to the plane of isotropy

For an isotropic material ($\nu' = \nu$, $E' = E$ and $G' = G$), Equation B8 reduces to the familiar form (Hooke's law):

$$\left.\begin{aligned} \varepsilon_{11} &= \frac{1}{E}(\sigma_{11} - \nu\sigma_{22} - \nu\sigma_{33}) \\ \varepsilon_{22} &= \frac{1}{E}(-\nu\sigma_{11} + \sigma_{22} - \nu\sigma_{33}) \\ \varepsilon_{33} &= \frac{1}{E}(-\nu\sigma_{11} - \nu\sigma_{22} + \sigma_{33}) \\ \varepsilon_{12} &= \frac{1}{2G}\sigma_{12} \\ \varepsilon_{13} &= \frac{1}{2G}\sigma_{13} \\ \varepsilon_{23} &= \frac{1}{2G}\sigma_{23} \end{aligned}\right\} \qquad \text{(B10)}$$

and the complementary energy function (Equation B4) takes the form

$$\bar{W} = \frac{J_1^2}{18K} + \frac{\bar{J}_2}{2G} \tag{B11}$$

where

J_1 = the first invariant of the stress tensor

$\bar{J}_2$ = the second invariant of the stress deviation tensor = $1/2\ S_{ij}\ S_{ij}$

S_{ij} = the stress deviation tensor

K = the bulk modulus of the material

G = the shear modulus of the material

Equation B10 can then be written in tensorial form as

$$\epsilon_{ij} = \frac{\partial \bar{W}}{\partial \sigma_{ij}} = \frac{1}{9K} J_1\ \delta_{ij} + \frac{1}{2G} S_{ij} \tag{B12}$$

where

$$\delta_{ij} = \text{Kronecker delta} = \begin{cases} 1, & i = j \\ 0, & i \neq j \end{cases}$$

7. Equation B12 expresses the strain tensor in terms of the first invariant of the stress tensor and the stress deviation tensor. This form of stress-strain relation is very convenient for use in a finite-difference or finite-element code calculation of a boundary-value problem. The objective of this section is to find a constitutive relation similar to Equation B12 for linear elastic transverse-isotropic materials. This can be done by defining the complementary energy function, Ω, in a form analogous to that of Equation B11; i.e.,

$$\Omega = \frac{\left(\phi_1^E\right)^2}{18B} + \frac{\phi_2^E}{2S} \tag{B13}$$

where[8]

ϕ_1^E = elastic pseudo invariant analogous to J_1

$= \sigma_{11} + \alpha^E(\sigma_{22} + \sigma_{33})$

$$\phi_2^E = \text{elastic pseudo invariant analogous to } \bar{J}_2$$
$$= \beta^E/6\,[(\sigma_{11} - \sigma_{22})^2 + (\sigma_{11} - \sigma_{33})^2] + (\sigma_{22} - \sigma_{33})^2/6$$
$$+ \gamma^E\,(\sigma_{12}{}^2 + \sigma_{13}{}^2) + (2 + \beta^E)\,\sigma_{23}^2/3$$

B , S , α^E , β^E and γ^E in the above equations are five independent material parameters that fully describe a linear elastic transverse-isotropic medium. The strain-stress relations for this material can be easily obtained from Equation B13 as

$$\varepsilon_{ij} = \frac{\partial \Omega}{\partial \sigma_{ij}} = \frac{1}{9B}\,\phi_1^E\,A_{ij}^E + \frac{1}{2S}\,\eta_{ij}^E \tag{B14}$$

where

$$\left[A_{ij}^E\right] = \text{a material property matrix} = \begin{bmatrix} 1 & 0 & 0 \\ 0 & \alpha^E & 0 \\ 0 & 0 & \alpha^E \end{bmatrix}$$

$$\eta_{ij}^E = \frac{\partial \phi_2^E}{\partial \sigma_{ij}}\,, \quad \eta_{ij}^E = \eta_{ji}^E \quad \text{and} \quad \eta_{ii}^E = 0$$

The term η_{ij}^E is a pseudo stress deviation tensor and can be related to the stresses as

$$\left.\begin{aligned}
\eta_{11}^E &= \frac{\beta^E}{3}\,(2\sigma_{11} - \sigma_{22} - \sigma_{33}) \\
\eta_{22}^E &= -\frac{\beta^3}{3}\,(\sigma_{11} - \sigma_{22}) + \frac{1}{3}\,(\sigma_{22} - \sigma_{33}) \\
\eta_{33}^E &= -\frac{\beta^E}{3}\,(\sigma_{11} - \sigma_{33}) - \frac{1}{3}\,(\sigma_{22} - \sigma_{33}) \\
\eta_{12}^E &= \gamma^E\,\sigma_{12} \\
\eta_{13}^E &= \gamma^E\,\sigma_{13} \\
\eta_{23}^E &= \left(\frac{2 + \beta^E}{3}\right)\sigma_{23}
\end{aligned}\right\} \tag{B15}$$

8. Note that Equation B14, the general constitutive equation for a linear elastic transverse-isotropic material, has a form analogous to that of Equation B12. In fact, when $\alpha^E = \beta^E = \gamma^E = 1$, Equation B14 reduces to the isotropic relation, Equation B12; i.e., ϕ_1^E becomes J_1, ϕ_2^E becomes $\bar{J}_2$, Ω becomes $\bar{W}$, A_{ij}^E becomes δ_{ij}, B becomes K (the bulk modulus of the material), and S becomes G (the shear modulus of the material).

9. By use of Equations B14 and B15, strain-stress relations analogous to Equation B8 can be written as

$$\left.\begin{aligned}
\varepsilon_{11} &= \left(\frac{1}{9B} + \frac{\beta^E}{3S}\right)\sigma_{11} + \left(\frac{\alpha^E}{9B} - \frac{\beta^E}{6S}\right)\sigma_{22} + \left(\frac{\alpha^E}{9B} - \frac{\beta^E}{6S}\right)\sigma_{33} \\
\varepsilon_{22} &= \left(\frac{\alpha^E}{9B} - \frac{\beta^E}{6S}\right)\sigma_{11} + \left[\frac{(\alpha^E)^2}{9B} + \frac{\beta^E + 1}{6S}\right]\sigma_{22} + \left[\frac{(\alpha^E)^2}{9B} - \frac{1}{6S}\right]\sigma_{33} \\
\varepsilon_{33} &= \left(\frac{\alpha^E}{9B} - \frac{\beta^E}{6S}\right)\sigma_{11} + \left[\frac{(\alpha^E)^2}{9B} - \frac{1}{6S}\right]\sigma_{22} + \left[\frac{(\alpha^E)^2}{9B} + \frac{\beta^E + 1}{6S}\right]\sigma_{33} \\
\varepsilon_{12} &= \frac{\gamma^E}{2S}\sigma_{12} \\
\varepsilon_{13} &= \frac{\gamma^E}{2S}\sigma_{13} \\
\varepsilon_{23} &= \left(\frac{2 + \beta^E}{6S}\right)\sigma_{23}
\end{aligned}\right\} \quad \text{(B16)}$$

A comparison of Equations B8 and B16 indicates that the following relations hold between the five independent material parameters, B, S, α^E, β^F, γ^E, and the customary independent material parameters, E, E', ν, ν' and G' (and the dependent parameter, G):

$$
\left.
\begin{aligned}
\alpha^E &= \frac{E'(1-\nu)}{E(1-2\nu')} - \frac{\nu'}{1-2\nu'} \\
\beta^E &= \frac{2\left(\frac{E'}{E}\right)^2(1-\nu^2) + (1+\nu)(1-4\nu')\frac{E'}{E}}{\left[\frac{E'}{E}(1-\nu)-\nu'\right]^2 + \nu\frac{E'}{E}\left[2\frac{E'}{E}(1-\nu)+1-4\nu'\right]} - 2 \\
\gamma^E &= \frac{2\frac{(E')^2}{EG'}(1-\nu) + (1-4\nu')\frac{E'}{G'}}{6\left[\frac{E'}{E}(1-\nu)-\nu'\right]^2 + 6\nu\frac{E'}{E}\left[2\frac{E'}{E}(1-\nu)+1-4\nu'\right]} \\
B &= \frac{\frac{2(E')^2}{9E}(1-\nu) + \frac{E'}{9}(1-4\nu')}{(1-2\nu')^2} \\
S &= \frac{2\frac{(E')^2}{E}(1-\nu) + E'(1-4\nu')}{6\left[\frac{E'}{E}(1-\nu)-\nu'\right]^2 + 6\nu\frac{E'}{E}\left[2\frac{E'}{E}(1-\nu)+1-4\nu'\right]}
\end{aligned}
\right\} \quad \text{(B17)}
$$

Equation B17 can be inverted to give

$$
\left.
\begin{aligned}
E' &= \frac{9BS}{3B\,\beta^E + S} \\
E &= \frac{18BS}{3B(\beta^E+1) + 2S(\alpha^E)^2} \\
\nu &= \frac{3B - 2S(\alpha^E)^2}{3B(\beta^E+1) + 2S(\alpha^E)^2} \\
\nu' &= \frac{3B\,\beta^E - 2S\,\alpha^E}{6B\,\beta^E + 2S} \\
G' &= \frac{S}{\gamma^E} \\
G &= \frac{3S}{2+\beta^E}
\end{aligned}
\right\} \quad \text{(B18)}
$$

Accordingly, conditions B9 become

$$\left.\begin{aligned}
\frac{9BS}{3B\,\beta^E + S} &> 0 \\
\frac{18BS}{3B\,(\beta^E + 1) + 2S\,(\alpha^E)^2} &> 0 \\
\frac{S}{\gamma^E} &> 0 \\
\frac{3S}{\beta^E + 2} &> 0 \\
-1 < \frac{3B - 2S\,(\alpha^E)^2}{3B\,(\beta^E + 1) + 2S\,(\alpha^E)^2} &< 1 \\
\frac{3B\,\beta^E + 4S\,(\alpha^E)^2}{6B\,\beta^E + 2S} - 2\left(\frac{3B\,\beta^E - 2S\,\alpha^E}{6B\,\beta^E + 2S}\right)^2 &> 0
\end{aligned}\right\} \qquad \text{(B19)}$$

As was pointed out previously, when $\alpha^E = \beta^E = \gamma^E = 1$, B becomes K (the bulk modulus of the material), S becomes G (the shear modulus of the material) and Equation B18 reduces to the following well known relations:

$$\left.\begin{aligned}
E = E' &= \frac{9BS}{3B + S} = \frac{9KG}{3K + G} \\
\nu = \nu' &= \frac{3B - 2S}{2(3B + S)} = \frac{3K - 2G}{2(3K + G)}
\end{aligned}\right\} \qquad \text{(B20)}$$

10. For the convenience of the reader, the bulk modulus of the transverse-isotropic material, K, the constrained modulus in the plane of isotropy, M, and the constrained modulus in a plane normal to the plane of isotropy, M', can be determined from the strain-stress relation (Equation B14) as

$$\left.\begin{aligned} K &= \frac{9B}{(1 + 2\alpha^E)^2} \\ M &= \frac{9B}{(1 + 2\alpha^E)^2} + \frac{12\,\alpha^E\,\beta^E\,(1 + \alpha^E) + 6(1 + \beta^E)}{\beta^E\,(1 + 2\alpha^E)^2\,(2 + \beta^E)}\,S \\ M' &= \frac{9B}{(1 + 2\alpha^E)^2} + \frac{12(\alpha^E)^2}{\beta^E\,(1 + 2\alpha^E)^2}\,S \end{aligned}\right\} \qquad \text{(B21)}$$

11. It is sometimes convenient to write Equation B14 in terms of hydrostatic and deviatoric components of strain; i.e.,

$$\left.\begin{aligned} \varepsilon_{kk} &= \frac{1 + 2\alpha^E}{9B}\,\phi_1^E \\ \bar{e}_{ij} &= \frac{1}{2S}\,\frac{\partial \phi_2^E}{\partial \sigma_{ij}} \end{aligned}\right\} \qquad \text{(B22)}$$

where

ε_{kk} = first invariant of the strain tensor

$\bar{e}_{ij}$ = pseudo strain deviator tensor

Hence, the total strain, ε_{ij}, becomes

$$\varepsilon_{ij} = \frac{\varepsilon_{kk}}{1 + 2\alpha^E}\,A_{ij}^E + \bar{e}_{ij} \qquad \text{(B23)}$$

The pseudo strain deviator tensor, $\bar{e}_{ij}$, is related to the strain deviator tensor, e_{ij}, as follows:

$$\bar{e}_{ij} = e_{ij} + \left(\frac{\delta_{ij}}{3} - \frac{A_{ij}^E}{1 + 2\alpha^E}\right)\varepsilon_{kk} \qquad \text{(B24)}$$

Equations B22 through B24 indicate that α^E and B are compressibility-related material properties, and that β^E, γ^E, and S are shear-related material properties.

12. With a clear understanding of the above general constitutive relationships for a linear elastic transverse-isotropic model, the derivation of a corresponding elastic-plastic transverse-isotropic model should be easy to follow.

APPENDIX C: GENERAL DESCRIPTION OF ELASTIC-PLASTIC CONSTITUTIVE MODELS

Introduction

1. The basic premise of elastic-plastic constitutive models is the assumption that certain materials are capable of undergoing small plastic (permanent) as well as elastic (recoverable) strains at each loading increment. Mathematically, the total strain increment is assumed to be the sum of the elastic and plastic strain increments; i.e.,

$$d\varepsilon_{ij} = d\varepsilon^{E}_{ij} + d\varepsilon^{P}_{ij} \tag{C1}$$

where

$d\varepsilon_{ij}$ = components of the total strain increment tensor

$d\varepsilon^{E}_{ij}$ = components of the elastic strain increment tensor

$d\varepsilon^{P}_{ij}$ = components of the plastic strain increment tensor

2. Within the elastic range, the behavior of the material can be described by an elastic constitutive relation similar to Equation B1:

$$d\varepsilon^{E}_{ij} = \bar{C}_{ijk\ell}\,(\sigma_{mn})\,d\sigma_{k\ell} \tag{C2}$$

where

$d\sigma_{k\ell}$ = components of the stress increment tensor

The behavior of the material in the plastic range can be described within the framework of the generalized incremental theory of plasticity. The mathematical basis of the theory was established by Drucker[19] who introduced the concept of material stability, which has the following implications:

a. Yield surface (loading function) should be convex in stress space.

b. Yield surface and plastic potential should coincide (which results in an "associated" flow rule).

c. Work-softening should not occur.

These three conditions can be summarized mathematically by the following inequality:

$$d\sigma_{ij}\ d\varepsilon^{P}_{ij} \geq 0 \tag{C3}$$

The above-mentioned conditions allow considerable flexibility in the choice of the form of the loading funciton, f, for the model, which serves as both a yield surface and the plastic potential. In general, the yield surface may be expressed as

$$f\ (\sigma_{ij}\ ,\ \kappa) = 0 \tag{C4}$$

The hardening parameter, κ, generally can be taken to be a function of the plastic strain tensor, ε^{P}_{ij}. The yield surface of Equation C4 may expand or contract as κ increases or decreases, respectively.

3. Conditions a, b, and c above, taken in conjunction with Equation C4, result in the following plastic flow rule for isotropic materials:

$$d\varepsilon^{P}_{ij} = \begin{cases} d\lambda\ \dfrac{\partial f}{\partial \sigma_{ij}} & \text{if } f = 0 \\ 0 & \text{if } f < 0 \end{cases} \tag{C5}$$

where $d\lambda$ is a positive scalar factor of proportionality, which is nonzero only when plastic deformations occur, and is dependent on the particular form of the loading function.

Derivation of Elastic-Plastic Transverse-Isotropic Constitutive Relations

4. Within the yield surface, f, the material behavior is transverse-isotropic elastic. In view of Equation B14, the elastic strain increment tensor, $d\varepsilon^{E}_{ij}$, takes the following from:

$$d\varepsilon^{E}_{ij} = \frac{1}{9B}\ d\phi^{E}_{1}\ A^{E}_{ij} + \frac{1}{2S}\ d\eta^{E}_{ij} \tag{C6}$$

in which

$$\eta^E_{ij} = \frac{\partial \phi^E_2}{\partial \sigma_{ij}}, \quad \eta^E_{ij} = \eta^E_{ji}, \quad \text{and} \quad \eta^E_{ii} = 0 \tag{C7}$$

where η^E_{ij} is the pseudo stress deviation tensor (Equation B15), and

$$A^E_{ij} = \begin{bmatrix} 1 & 0 & 0 \\ 0 & \alpha^E & 0 \\ 0 & 0 & \alpha^E \end{bmatrix} \tag{C8}$$

The elastic behavior is governed by the three elastic constants, α^E, β^E, and γ^E, and by the two response functions, B and S. In order to introduce nonlinear behavior in the elastic range, the response functions may be expressed as

$$\left.\begin{aligned} B &= B\left(\phi^E_1, \kappa\right) \\ S &= S\left(\sqrt{\phi^E_2}, \kappa\right) \end{aligned}\right\} \tag{C9}$$

Note that in view of the existence of the complementary energy function Ω (Equation B13), the model is path indenpendent during purely elastic deformation.[7,20]

5. The hydrostatic and deviatoric components of strain can be easily obtained from Equation C6, respectively, as

$$d\varepsilon^E_{kk} = \frac{1 + 2\alpha^E}{9B}\, d\phi^E_1 \tag{C10}$$

and

$$d\bar{e}^E_{ij} = \frac{1}{2S}\, d\eta^E_{ij} \tag{C11}$$

where $d\varepsilon^E_{kk}$ is the increment of elastic volumetric strain and $d\bar{e}^E_{ij}$ is the pseudo elastic strain deviation increment tensor. The elastic

strain deviation increment tensor, de^E_{ij}, is related to $d\bar{e}^E_{ij}$ through the following relation (see Equation B24):

$$de^E_{ij} = d\bar{e}^E_{ij} - \left(\frac{\delta_{ij}}{3} - \frac{A^E_{ij}}{1 + 2\alpha^E}\right) d\epsilon^E_{kk} \tag{C12}$$

Note that when $\alpha^E = \beta^E = \gamma^E = 1$, the above equations reduce to their isotropic counterparts and the response functions, B and S, become the isotropic bulk and shear modulus response functions, respectively.

6. The plastic strain increment tensor is given by Equation C5 where the loading function f may be expressed as (Figure C1)

$$f\left(\phi^P_1, \sqrt{\phi^P_2}, \kappa\right) = 0 \tag{C13}$$

in which ϕ^P_1 and ϕ^P_2 are defined similarly to ϕ^E_1 and ϕ^E_2 (Equation B13):

$$\left.\begin{aligned} \phi^P_1 &= \sigma_{11} + \alpha^P\left(\sigma_{22} + \sigma_{33}\right) \\ \phi^P_2 &= \frac{\beta^P}{6}\left[\left(\sigma_{11} - \sigma_{22}\right)^2 + \left(\sigma_{11} - \sigma_{33}\right)^2\right] \\ &\quad + \frac{\left(\sigma_{22} - \sigma_{33}\right)^2}{6} + \gamma^P\left(\sigma_{12}{}^2 + \sigma_{13}{}^2\right) + \left(\frac{2 + \beta^P}{3}\right)\sigma_{23}{}^2 \end{aligned}\right\} \tag{C14}$$

The hardening parameter κ can be one of the following functions:

$$\kappa = g_1\left(\epsilon^P_{kk}\right) \tag{C15}$$

$$\kappa = g_2\left[\left(\epsilon^P_{kk}\right)_{max}\right] \tag{C16}$$

The use of Equation C15 permits the hardening surface to move back toward the origin (Figure C1) when a point on the failure envelope is reached (which produces dilatancy of the material). This feature of the model is useful for controlling the amount of dilatancy that can occur. The use of Equation C16, on the other hand, only permits the hardening surface to move away from the origin, thus ensuring full dilatancy on the failure envelope while still permitting hysteresis in a hydrostatic load-unload cycle.

7. The plastic loading criteria for the function f are given by

$$\frac{\partial f}{\partial \sigma_{ij}} d\sigma_{ij} \begin{cases} > 0 \text{ loading} \\ = 0 \text{ neutral loading} \\ < 0 \text{ unloading} \end{cases} \qquad \text{(C17)}$$

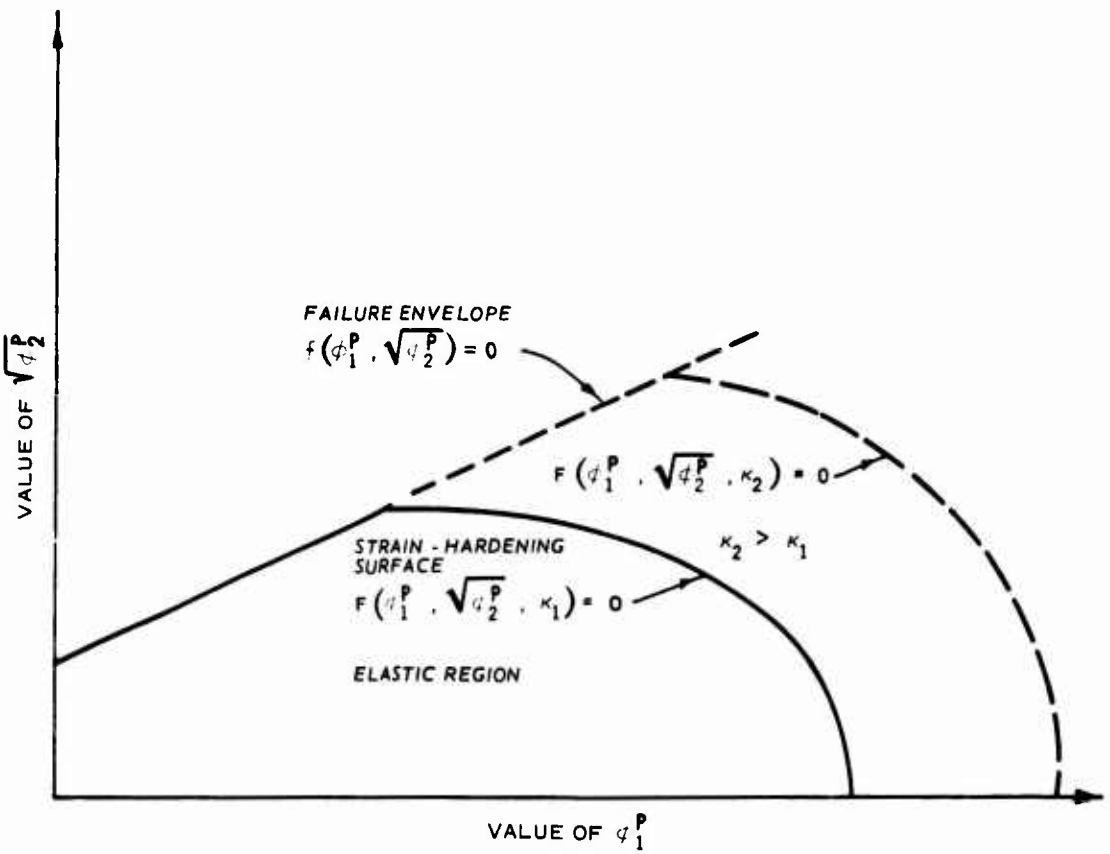

Figure C1. Typical yield surface for transverse-isotropic elastic-plastic model

Plastic strains will occur only when $d\mathcal{f}$ is positive and $\mathcal{f} = 0$. During unloading or neutral loading, as well as for $\mathcal{f} < 0$, the material will behave elastically. The prescription that neutral loading produces no plastic strain is called the "continuity condition." Its satisfaction leads to coincidence of the elastic and plastic constitutive laws during neutral loading.[19,21]

8. As with the elastic relation, the plastic stress-strain relation can be expressed in terms of the hydrostatic and deviatoric components of strain. Application of the chain rule of differentiation to the right side of Equation C5 yields

$$d\varepsilon_{ij}^{P} = d\lambda \left[\frac{\partial \mathcal{f}}{\partial \phi_1^P} \frac{\partial \phi_1^P}{\partial \sigma_{ij}} + \frac{\partial \mathcal{f}}{\partial \sqrt{\phi_2^P}} \frac{\partial \sqrt{\phi_2^P}}{\partial \sigma_{ij}} \right]$$

or

$$d\varepsilon_{ij}^{P} = d\lambda \left[\frac{\partial \mathcal{f}}{\partial \phi_1^P} A_{ij}^{P} + \frac{1}{2\sqrt{\phi_2^P}} \frac{\partial \mathcal{f}}{\partial \sqrt{\phi_2^P}} \eta_{ij}^{P} \right] \tag{C18}$$

where

$$A_{ij}^{P} = \begin{bmatrix} 1 & 0 & 0 \\ 0 & \alpha^P & 0 \\ 0 & 0 & \alpha^P \end{bmatrix} \tag{C19}$$

and

$$\eta_{ij}^{P} = \frac{\partial \phi_2^P}{\partial \sigma_{ij}} \text{ and } \eta_{ii}^{P} = 0 \tag{C20}$$

Both sides of Equation C18 are multiplied by the Kronecker delta, δ_{ij}, to give

$$d\varepsilon_{kk}^{P} = d\lambda \, (1 + 2\alpha^P) \frac{\partial \mathcal{f}}{\partial \phi_1^P} \tag{C21}$$

The pseudo plastic strain deviation increment tensor, $d\bar{e}^P_{ij}$, can be written as

$$d\bar{e}^P_{ij} = d\varepsilon^P_{ij} - \frac{d\varepsilon^P_{kk}}{(1 + 2\alpha^P)} A^P_{ij} \tag{C22}$$

Substitution of Equations C18 and C21 into Equation C22 yields

$$d\bar{e}^P_{ij} = \frac{d\lambda}{2\sqrt{\phi^P_2}} \frac{\partial f}{\partial \sqrt{\phi^P_2}} \eta^P_{ij} \tag{C23}$$

but, analogously to Equation C12, the plastic strain deviation increment tensor, de^P_{ij}, can be written as

$$de^P_{ij} = d\bar{e}^P_{ij} - \left(\frac{\delta_{ij}}{3} - \frac{A^P_{ij}}{1 + 2\alpha^P} \right) d\varepsilon^P_{kk} \tag{C24}$$

Consequently, substitution of Equations C21 and C23 into Equation C24, leads to

$$de^P_{ij} = d\lambda \left[\frac{1}{2\sqrt{\phi^P_2}} \frac{\partial f}{\partial \sqrt{\phi^P_2}} \eta^P_{ij} + \left(A^P_{ij} - \frac{1 + 2\alpha^P}{3} \delta_{ij} \right) \frac{\partial f}{\partial \phi^P_1} \right] \tag{C25}$$

9. To use Equations C18 through C25, the proportionality factor, $d\lambda$, must be determined. This can be accomplished in the following manner. From Equations C13 and C15 or C16 the total derivative of f becomes

$$df = \frac{\partial f}{\partial \phi^P_1} d\phi^P_1 + \frac{1}{2\sqrt{\phi^P_2}} \frac{\partial f}{\partial \sqrt{\phi^P_2}} d\phi^P_2 + \frac{\partial f}{\partial \kappa} \frac{\partial \kappa}{\partial \varepsilon^P_{kk}} d\varepsilon^P_{kk} = 0 \tag{C26}$$

The values of $d\phi_1^P$ and $d\phi_2^P$ in terms of $d\phi_1^E$, η_{ij}^E, and η_{ij}^P can be obtained from Equations B13, B15, and C14 as

$$d\phi_1^P = \left(\frac{1 + 2\alpha^P}{1 + 2\alpha^E}\right) d\phi_1^E - \frac{3(\alpha^P - \alpha^E)}{\beta^E(1 + 2\alpha^E)} d\eta_{11}^E \tag{C27}$$

$$d\phi_2^P = \frac{3}{\beta^E(2 + \beta^E)} \eta_{11}^P \, d\eta_{11}^E + \frac{3}{2 + \beta^E} \left[\eta_{22}^P \, d\eta_{22}^E + \eta_{33}^P \, d\eta_{33}^E\right]$$

$$+ \frac{2}{\gamma^E} \left[\eta_{12}^P \, d\eta_{12}^E + \eta_{13}^P \, d\eta_{13}^E\right] + \left(\frac{6}{2 + \beta^E}\right) \eta_{23}^P \, d\eta_{23}^E \tag{C28}$$

In view of Equations C10 and C11, Equations C27 and C28 become

$$d\phi_1^P = 9B \frac{(1 + 2\alpha^P)}{(1 + 2\alpha^E)^2} d\varepsilon_{kk}^E - \frac{6S(\alpha^P - \alpha^E)}{\beta^E(1 + 2\alpha^E)} d\bar{e}_{11}^E \tag{C29}$$

$$d\phi_2^P = \frac{6S}{\beta^E(2 + \beta^E)} \eta_{11}^P \, d\bar{e}_{11}^E + \frac{6S}{(2 + \beta^E)} \left[\eta_{22}^P \, d\bar{e}_{22}^E + \eta_{33}^P \, d\bar{e}_{33}^E\right]$$

$$+ \frac{4S}{\gamma^E} \left[\eta_{12}^P \, d\bar{e}_{12}^E + \eta_{13}^P \, d\bar{e}_{13}^E\right] + \frac{12S}{(2 + \beta^E)} \eta_{23}^P \, d\bar{e}_{23}^E \tag{C30}$$

The relationship between $d\varepsilon_{ij}$, $d\varepsilon_{kk}$, de_{ij}, $d\varepsilon_{kk}^E$, $d\varepsilon_{kk}^P$, $d\bar{e}_{ij}^E$, and $d\bar{e}_{ij}^P$ can be easily obtained from Equations C1, C6 through C12, C22, and C24 as

$$d\varepsilon_{ij} = d\bar{e}_{ij}^E + d\bar{e}_{ij}^P + \frac{A_{ij}^E}{1 + 2\alpha^E} d\varepsilon_{kk}^E + \frac{A_{ij}^P}{1 + 2\alpha^P} d\varepsilon_{kk}^P \tag{C31}$$

and

$$de_{ij} = d\bar{e}_{ij}^E + d\bar{e}_{ij}^P + \left(\frac{A_{ij}^E}{1 + 2\alpha^E} - \frac{\delta_{ij}}{3}\right) d\varepsilon_{kk} + \left(\frac{A_{ij}^P}{1 + 2\alpha^P} - \frac{A_{ij}^E}{1 + 2\alpha^E}\right) d\varepsilon_{kk}^P \tag{C32}$$

The substitution of Equations C31 and C32 into Equations C29 and C30 results in

$$d\phi_1^P = \left[9B \frac{(1 + 2\alpha^P)}{(1 + 2\alpha^E)^2} - \frac{4S(\alpha^P - \alpha^E)(\alpha^E - 1)}{\beta^E(1 + 2\alpha^E)^2} \right] d\varepsilon_{kk}$$

$$- \frac{6S(\alpha^P - \alpha^E)}{\beta^E(1 + 2\alpha^E)} de_{11} + \frac{6S(\alpha^P - \alpha^E)}{\beta^E(1 + 2\alpha^E)} \bar{de}_{11}^P$$

$$- \left[9B \frac{(1 + 2\alpha^P)}{(1 + 2\alpha^E)^2} + \frac{12S(\alpha^P - \alpha^E)^2}{\beta^E(1 + 2\alpha^P)(1 - 2\alpha^E)^2} \right] d\varepsilon_{kk}^P \qquad (C33)$$

and

$$d\phi_2^P = \frac{2S}{\beta^E} \left(\frac{\alpha^E - 1}{1 + 2\alpha^E} \right) \eta_{11}^P \, d\varepsilon_{kk} + \frac{6S}{\beta^E(2 + \beta^E)} \eta_{11}^P \, de_{11}$$

$$+ \frac{6S}{(2 + \beta^E)} \left[\eta_{22}^P \, de_{22} + \eta_{33}^P \, de_{33} \right] + \frac{4S}{\gamma^E} \left[\eta_{12}^P \, de_{12} + \eta_{13}^P \, de_{13} \right]$$

$$+ \left(\frac{12S}{2 + \beta^E} \right) \eta_{23}^P \, de_{23} + \frac{6S}{\beta^E} \frac{\alpha^P - \alpha^E}{(1 + 2\alpha^E)(1 + 2\alpha^P)} \eta_{11}^P \, d\varepsilon_{kk}^P$$

$$- \frac{6S}{\beta^E(2 + \beta^E)} \eta_{11}^P \, \bar{de}_{11}^P - \frac{6S}{(2 + \beta^E)} \left[\eta_{22}^P \, \bar{de}_{22}^P + \eta_{33}^P \, \bar{de}_{33}^P \right]$$

$$- \frac{4S}{\gamma^E} \left[\eta_{12}^P \, \bar{de}_{12}^P + \eta_{13}^P \, \bar{de}_{13}^P \right] - \frac{12S}{(2 + \beta^E)} \eta_{23}^P \, \bar{de}_{23}^P \qquad (C34)$$

Substitution of Equations C21 and C23 into the above two equations gives

$$d\phi_1^P = \left[9B\frac{(1+2\alpha^P)}{(1+2\alpha^E)^2} - \frac{4S(\alpha^P-\alpha^E)(\alpha^E-1)}{\beta^E(1+2\alpha^E)^2}\right] d\epsilon_{kk} - \frac{6S(\alpha^P-\alpha^E)}{\beta^E(1+2\alpha^E)} de_{11}$$

$$- \left[9B\left(\frac{1+2\alpha^P}{1+2\alpha^E}\right)^2 + \frac{12S(\alpha^P-\alpha^E)^2}{\beta^E(1+2\alpha^E)^2}\right] d\lambda \frac{\partial f}{\partial \phi_1^P}$$

$$+ \frac{3S(\alpha^P-\alpha^E)}{\beta^E(1+2\alpha^E)} \frac{d\lambda}{\sqrt{\phi_2^P}} \frac{\partial f}{\partial \sqrt{\phi_2^P}} \eta_{11}^P \qquad (C35)$$

and

$$d\phi_2^P = \frac{2S}{\beta^E}\left(\frac{\alpha^E-1}{1+2\alpha^E}\right) \eta_{11}^P\, d\epsilon_{kk} + \frac{6S}{\beta^E(2+\beta^E)} \eta_{11}^P\, de_{11}$$

$$+ \frac{6S}{(2+\beta^E)}\left[\eta_{22}^P\, de_{22} + \eta_{33}^P\, de_{33}\right] + \frac{4S}{\gamma^E}\left[\eta_{12}^P\, de_{12} + \eta_{13}^P\, de_{13}\right]$$

$$+ \left(\frac{12S}{2+\beta^E}\right)\eta_{23}^P\, de_{23} + \frac{6S}{\beta^E}\left(\frac{\alpha^P-\alpha^E}{1+2\alpha^E}\right) d\lambda\, \eta_{11}^P \frac{\partial f}{\partial \phi_1^P}$$

$$- \frac{3S}{\beta^E(2+\beta^E)} \frac{d\lambda}{\sqrt{\phi_2^P}} \left(\eta_{11}^P\right)^2 \frac{\partial f}{\partial \sqrt{\phi_2^P}} - \frac{3S}{(2+\beta^E)} \frac{d\lambda}{\sqrt{\phi_2^P}} \left[\left(\eta_{22}^P\right)^2 + \left(\eta_{33}^P\right)^2\right] \frac{\partial f}{\partial \sqrt{\phi_2^P}}$$

$$- \frac{2S}{\gamma^E} \frac{d\lambda}{\sqrt{\phi_2^P}} \left[\left(\eta_{12}^P\right)^2 + \left(\eta_{13}^P\right)^2\right] \frac{\partial f}{\partial \sqrt{\phi_2^P}} - \frac{6S}{(2+\beta^E)} \frac{d\lambda}{\sqrt{\phi_2^P}} \left(\eta_{23}^P\right)^2 \frac{\partial f}{\partial \sqrt{\phi_2^P}} \qquad (C36)$$

when Equations C35 and C36 are substituted into Equation C26, which is solved for $d\lambda$, this produces

$$d\lambda = \frac{\Lambda}{\zeta} \tag{C37}$$

in which

$$\Lambda = \left[9B \frac{(1 + 2\alpha^P)}{(1 + 2\alpha^E)^2} \frac{\partial f}{\partial \phi_1^P} - \frac{4S(\alpha^P - \alpha^E)(\alpha^E - 1)}{\beta^E (1 + 2\alpha^E)^2} \frac{\partial f}{\partial \phi_1^E} \right.$$

$$\left. + \frac{S}{\beta^E \sqrt{\phi_2^P}} \left(\frac{\alpha^E - 1}{1 + 2\alpha^E} \right) \frac{\partial f}{\partial \sqrt{\phi_2^P}} \eta_{11}^P \right] d\varepsilon_{kk} - \frac{6S(\alpha^P - \alpha^E)}{\beta^E (1 + 2\alpha^E)} \frac{\partial f}{\partial \phi_1^P} \, de_{11}$$

$$+ \frac{3S}{2 + \beta^E} \left[\frac{1}{\beta^E} \eta_{11}^P \, de_{11} + \eta_{22}^P \, de_{22} + \eta_{33}^P \, de_{33} \right] \frac{1}{\sqrt{\phi_2^P}} \frac{\partial f}{\partial \sqrt{\phi_2^P}}$$

$$+ \frac{2S}{\gamma^E} \left[\eta_{12}^P \, de_{12} + \eta_{13}^P \, de_{13} \right] \frac{1}{\sqrt{\phi_2^P}} \frac{\partial f}{\partial \sqrt{\phi_2^P}}$$

$$+ \left(\frac{6S}{2 + \beta^E} \right) \frac{1}{\sqrt{\phi_2^P}} \eta_{23}^P \frac{\partial f}{\partial \sqrt{\phi_2^P}} \, de_{23} \tag{C38}$$

and

$$\zeta = \frac{1}{(1 + 2\alpha^E)^2} \left[9B(1 + 2\alpha^P)^2 + \frac{12S}{\beta^E} (\alpha^P - \alpha^E)^2 \right] \left(\frac{\partial f}{\partial \phi_1^P} \right)^2$$

$$- \frac{6S}{\beta^E} \left(\frac{\alpha^P - \alpha^E}{1 + 2\alpha^E} \right) \frac{1}{\sqrt{\phi_2^P}} \eta_{11}^P \frac{\partial f}{\partial \sqrt{\phi_2^P}} \frac{\partial f}{\partial \phi_1^P}$$

$$+ \frac{3S}{2(2 + \beta^E)} \frac{1}{\phi_2^P} \left(\frac{\partial f}{\partial \sqrt{\phi_2^P}} \right)^2 \left[\frac{1}{\beta^E} \left(\eta_{11}^P \right)^2 + \left(\eta_{22}^P \right)^2 + \left(\eta_{33}^P \right)^2 \right]$$

$$+ \frac{S}{\gamma^E} \frac{1}{\phi_2^P} \left(\frac{\partial f}{\partial \sqrt{\phi_2^P}} \right)^2 \left[\left(\eta_{12}^P \right)^2 + \left(\eta_{13}^P \right)^2 \right]$$

$$+ \left(\frac{3S}{2 + \beta^E} \right) \frac{1}{\phi_2^P} \left(\eta_{23}^P \right)^2 \left(\frac{\partial f}{\partial \sqrt{\phi_2^P}} \right)^2 - (1 + 2\alpha^P) \frac{\partial f}{\partial \phi_1^P} \frac{\partial f}{\partial \varepsilon_{kk}^P} \tag{C39}$$

10. The total strain increment tensor can be obtained by the combination of Equations C1, C6, C18, and C37; thus,

$$d\varepsilon_{ij} = \frac{1}{9B}\, d\phi_1^E\, A_{ij}^E + \frac{1}{2S}\, dn_{ij}^E + \frac{\Lambda}{\zeta}\left(\frac{\partial \zeta}{\partial \phi_1^P}\, A_{ij}^P + \frac{1}{2\sqrt{\phi_2^P}}\,\frac{\partial \zeta}{\partial \sqrt{\phi_2^P}}\, \eta_{ij}^P\right) \quad (C40)$$

Equation C40 is the general constitutive equation for an elastic-plastic transverse-isotropic material. To use these equations, it is only necessary to specify the functional forms of B, S, κ, and ζ and, of course, to determine experimentally the numerical values of the coefficients in these functions as well as the values of the parameters α^E, α^P, β^E, β^P, γ^E, and γ^P.

APPENDIX D: NOTATION

a_i	Components of acceleration vector
$\left[A^E_{ij}\right]$	Elastic material property matrix
$\left[A^P_{ij}\right]$	Plastic material property matrix
B	Elastic bulk response function
B_i	Initial value of the response function B
B_{max}	Maximum value of response function B
B_1, B_2	Material constants
$\bar{C}_{ijk\ell}$	Elastic compliances of the material
$d\bar{e}^E_{ij}$	Pseudo elastic strain deviation increment tensor
$d\varepsilon_{ij}$	Components of the total strain increment tensor
$d\varepsilon^E_{ij}$	Components of the elastic strain increment tensor
$d\varepsilon^P_{ij}$	Components of the plastic strain increment tensor
$d\varepsilon^E_{kk}$	Hydrostatic component of strain or volumetric strain
$d\lambda$	Positive scalar factor of proportionality; appears in the flow rule
$d\sigma_{ij}$	Components of the stress increment tensor
D	Material constant
D_{mn}	Deformation-rate tensor
e	Void ratio
e_{ij}	Strain deviation tensor
$\bar{e}_{ij}$	Pseudo strain deviation tensor
$\bar{e}^E_{ij}$	Elastic pseudo strain deviation tensor
$\bar{e}^P_{ij}$	Plastic pseudo strain deviation tensor
E	Young's modulus in the plane of isotropy
E'	Young's modulus in a plane normal to the plane of isotropy

f	Failure envelope
f	Loading function
F	Strain-hardening elliptic cap
F_i	Components of body force
$G = \frac{E}{2(1+\nu)}$	Shear modulus for the plane of isotropy
G'	Shear modulus for a plane normal to the plane of isotropy
J_1	First invariant of the stress tensor
J_1'	First invariant of the effective stress tensor
$\bar{J}_2$	Second invariant of the total stress deviation tensor
$J_2 = \bar{J}_2'$	Second invariant of the total or effective stress deviation tensor
k	Pseudo cohesive strength parameter of the material
K	Bulk modulus of the material
K_s	Bulk modulus of anisotropic material under drained hydrostatic unloading
$\tilde{K}_s$	Apparent bulk modulus of anisotropic material under drained hydrostatic unloading
$L(\kappa)$	Intersection of the hardening surface with the failure envelope $f\left(\emptyset_1^P , \sqrt{\emptyset_2^P}\right)$
m	Subscript used to indicate "mixture"
M	Constrained modulus in the plane of isotropy
M'	Constrained modulus in a plane normal to the plane of isotropy
P	Total mean normal stress
P'	Effective mean normal stress
P_a	Pore air pressure
P_c	Confining pressure at the end of the hydrostatic compression phase of a triaxial test
P_c'	Effective confining pressure at the end of the hydrostatic compression phase of a triaxial test

P_w	Pore water pressure
r_{qp}	Spin tensor
r,θ,z	Cylindrical coordinate system
R	Ratio of the major to minor axes of the elliptic hardening surface
R_i, R_1, R_2	Material constants
s	Subscript used to indicate "skeleton"
S	Elastic shear response function
S_i	Initial value of the response function S
S_{ij}	Stress deviation tensor
S_1, S_2, S_3, S_4	Material constants
t	Time
u	Pore pressure representing the combined effect of the pore air pressure and the pore water pressure
u_i	Displacement vector
v_i	Components of velocity vector
$\Delta V/V$	Volumetric strain
W	Maximum plastic volumetric compression that the material can experience under hydrostatic loading
$\overline{W}$	Complementary energy function for isotropic materials
X_i	Cartesian coordinate system
$X(\kappa)$	Intersection of the hardening surface with the ϕ_1^P axis
α^E	Material constant; appears in the definition of the first elastic pseudo invariant of stress
α^P	Material constant; appears in the definition of the first plastic pseudo invariant of stress
β^E	Material constant; appears in the definition of the second elastic pseudo invariant of stress
β^P	Material constant; appears in the definition of the second plastic pseudo invariant of stress

γ^E Material constant; appears in the definition of the second elastic pseudo invariant of stress

γ^P Material constant; appears in the definition of the second plastic pseudo invariant of stress

δ_{ij} Kronecker delta

ε_{ij} Total strain tensor

ε^E_{ij} Elastic strain tensor

ε^E_{kk} Elastic volumetric strain

ε^E_r Elastic radial strain component

ε^E_z Elastic vertical strain component

ε^E_θ Elastic tangential strain component

ε^E_{11} Elastic strain component normal to the plane of isotropy

ε^E_{13} Elastic shear strain component

ε^E_{22} or ε^E_{33} Elastic strain component in the plane of isotropy

ε_{kk} Total volumetric strain

ε^P_{ij} Plastic strain tensor

ε^P_{kk} Plastic volumetric strain

ε^P_r Plastic radial strain component

ε^P_z Plastic vertical strain component

ε^P_θ Plastic tangential strain component

ε^P_{11} Plastic strain component normal to the plane of isotropy

ε^P_{13} Plastic shear strain component

ε^P_{22} or ε^P_{33} Plastic strain component in the plane of isotropy

ε_r Total radial strain, strain in the plane of isotropy

ε_z Total vertical strain, strain normal to the plane of isotropy

ε_{11} Total strain normal to the plane of isotropy

ε_{13} Total shear strain

ε_{22} or ε_{33}	Total strain component in the plane of isotropy
η_{ij}^{E}	Elastic pseudo stress deviation tensor
η_{ij}^{P}	Plastic pseudo stress deviation tensor
κ	Hardening parameter
ν	Poisson's ratio that characterizes the transverse reduction in the plane of isotropy due to stress in the same plane
ν'	Poisson's ratio that characterizes the transverse reduction in the plane of isotropy due to the stress normal to it
ρ	Mass density
σ_{ij}	Total stress tensor
σ'_{ij}	Effective stress tensor
σ_r	Total radial stress
σ'_r	Effective radial stress
σ_z	Total axial stress
σ'_z	Effective axial stress
σ_θ	Total tangential stress
σ'_θ	Effective tangential stress
$\emptyset_1^E$	First elastic pseudo invariant of total stress
$\emptyset_1'^E$	First elastic pseudo invariant of effective stress
$\emptyset_2^E$	Second elastic pseudo invariant of total stress
$\emptyset_2'^E$	Second elastic pseudo invariant of effective stress
$\emptyset_1^P$	First plastic pseudo invariant of total stress
$\emptyset_1'^P$	First plastic pseudo invariant of effective stress
$\emptyset_2^P$	Second plastic pseudo invariant of total stress
$\emptyset_2'^P$	Second plastic pseudo invarinat of effective stress

χ Dimensionless quantity proportional to the pore volume occupied by the water phase

ψ Pseudo frictional strength parameter

Ω Complementary energy function for transverse-isotropic materials

In accordance with letter from DAEN-RDC, DAEN-ASI dated 22 July 1977, Subject: Facsimile Catalog Cards for Laboratory Technical Publications, a facsimile catalog card in Library of Congress MARC format is reproduced below.

Baladi, George Youssef
An elastic-plastic constitutive relation for transverse-isotropic three-phase earth materials / by George Y. Baladi. Vicksburg, Miss. : U. S. Waterways Experiment Station ; Springfield, Va. : available from National Technical Information Service, 1978.
48, [33] p. : ill. ; 27 cm. (Miscellaneous paper - U. S. Army Engineer Waterways Experiment Station ; S-78-14)
Sponsored by Assistant Secretary of the Army (R&D), Department of the Army, Washington, D. C., under Project No. 4A161101A91D.
References: p. 47-48.

1. Anisotropy. 2. Constitutive models. 3. Elastic media. 4. Elastic plastic behavior. 5. Saturated soils. 6. Stress-strain relations. 7. Three-phase media. 8. Transverse-isotropic materials. I. United States. Assistant Secretary of the Army (Research and Development). II. Series: United States. Waterways Experiment Station, Vicksburg, Miss. Miscellaneous paper ; S-78-14.
TA7.W34m no.S-78-14